telaprevir and MK-0608 were combined, the anti-HCV effect was increased without cellular damage (Fig. 2).

Effects of telaprevir and MK-0608 on HCV replication in vivo

To analyze the effect of telaprevir and MK-0608 *in vivo*, we used genotype 1b HCV-infected human hepatocyte chimeric mice. Eight HCV-infected mice were treated with either 200 mg/kg of telaprevir or 3 mg/kg of MK-0608 for 4 weeks. At the end of 1 week, treatment resulted in a 1.9 ± 0.7 log reduction of HCV RNA in telaprevir-treated mice and a 2.6 ± 0.2 log reduction in MK-0608-treated mice (Fig. 3A and C). During the treatment, the level of HSA did not decrease. Serum HCV RNA level rebounded in one of the four telaprevir-treated mice and in two of the three MK-0608-treated mice (a MK-0608-treated mouse died after 1 week of treatment). Nucleotide and amino acid sequence analysis showed the emergence of a V36A mutation (NS3-4A protease inhibitor-resistant variant) in the NS3 region (Fig. 3B) in a telaprevir-treated mouse, and a S282T mutation (NS5B polymerase inhibitor-resistant variant) in the NS5B region (Fig. 3D) in MK-0608-treated mice, similar to clinical observations and analysis using HCV-infected chimpanzees [22,23].

Combination treatment with telaprevir and MK-0608 on HCV replication in vivo

Because mono-therapy with either telaprevir or MK0608 resulted in emergence of drug-resistant variants, we analyzed the effect of

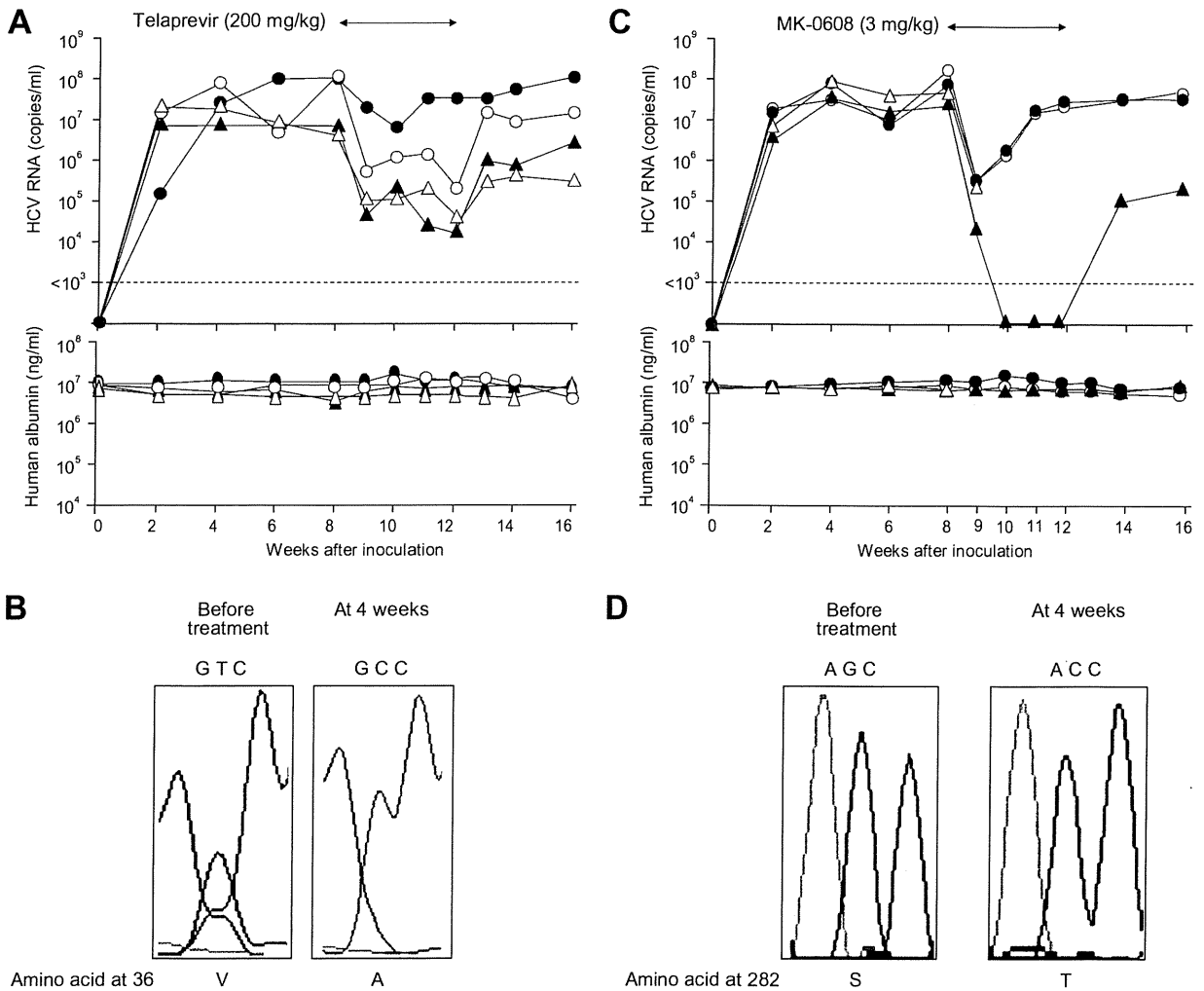

Fig. 3. Antiviral effects of either telaprevir or MK0608 monotherapy on HCV-infected mice. Mice were injected intravenously with 100 μl of HCV-positive human serum samples. Eight weeks after HCV infection, mice were treated with either 200 mg/kg of telaprevir (A) or 3 mg/kg of MK-0608 (C) for 4 weeks. Mice serum samples were obtained at the indicated times, and HCV RNA titer (upper panel) and human serum albumin concentration (lower panel) were analyzed. The horizontal dashed line represents the detection limit (10^3 copies/ml). Note that one telaprevir-treated mouse (A, closed circle) and two MK-0608-treated mice (B, closed circle and open circle) showed a viral breakthrough during the dosing period. Nucleotide and amino acid (aa) sequence analysis of aa 36 in the HCV NS3 (B) or at aa 282 in the NS5B region (D) by direct sequencing in mice serum samples obtained before treatment and at 4 weeks.

Research Article

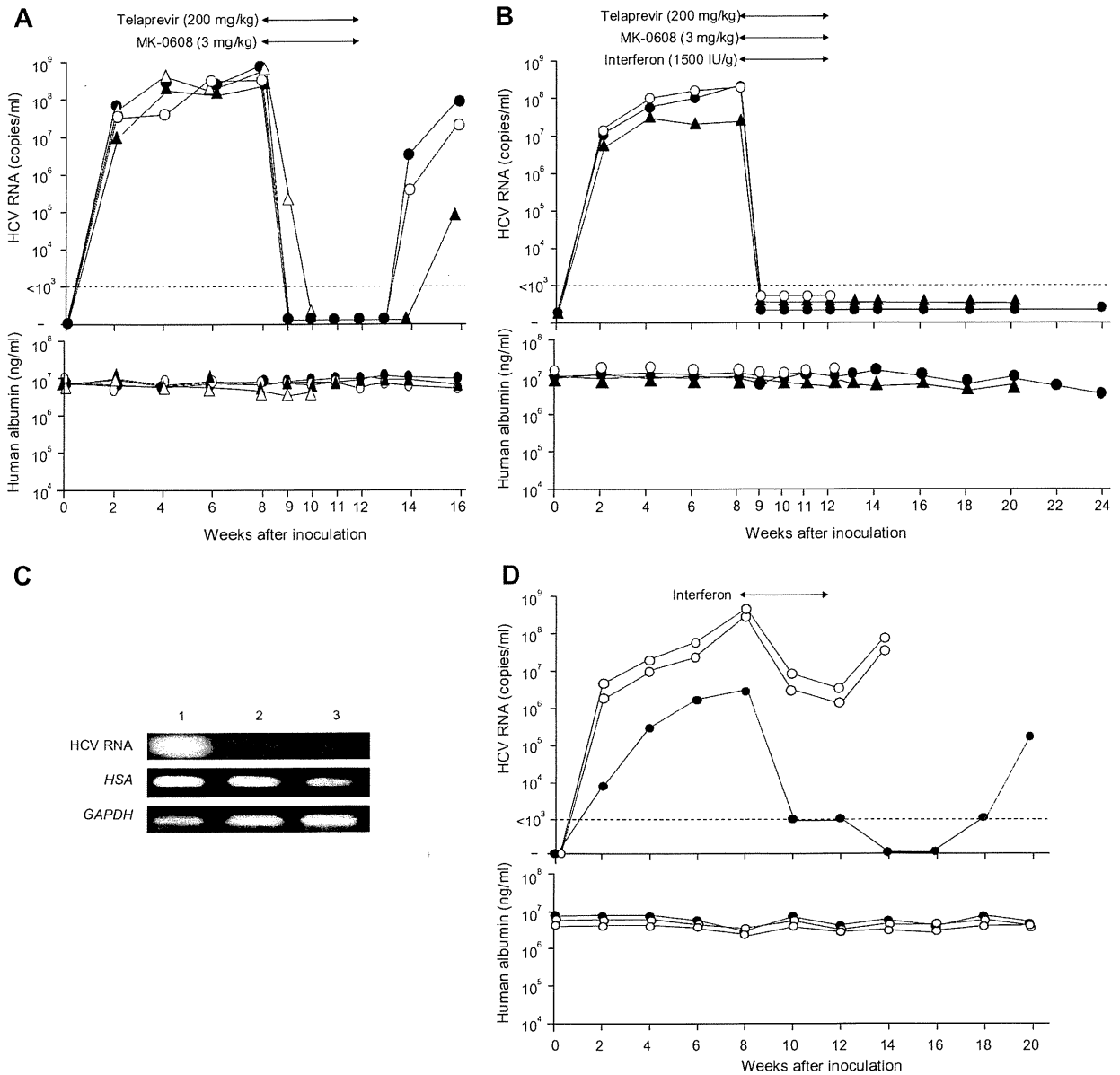

Fig. 4. Antiviral effect of combination treatment on HCV-infected mice. HCV-infected mice were treated with 200 mg/kg of telaprevir plus 3 mg/kg of MK-0608 without (A) or with (B) 1500 IU/g of human interferon-alpha for 4 weeks. Mice serum samples were obtained at the indicated times, and HCV RNA titer (upper panel) and human serum albumin concentration (lower panel) were analyzed. (C) Nested PCR of HCV RNA, human serum albumin (*HSA*) and *GAPDH* in a telaprevir, MK-0608 and interferon-alpha-treated mouse liver at 24 weeks (lane 2). Mice livers with (lane 1) or without (lane 3) HCV-infection were also analyzed. (D) HCV-infected mice were treated with either 1500 (open circles) or 7000 IU/g (closed circles) of interferon-alpha for 4 weeks.

combination treatment of these drugs with or without IFN on HCV replication *in vivo*. Four HCV-infected mice were treated with telaprevir plus MK-0608 for 4 weeks (Fig. 4A). Serum HCV RNA became negative by nested PCR with this combination treatment in all mice. One mouse died after 2 weeks of treatment. During the treatment, no emergence of resistant strains was observed in each of the remaining three mice; however, all mice became positive for HCV RNA again after cessation of the therapy. Another three mice were treated with telaprevir, MK-0608 and IFN-alpha for 4 weeks (Fig. 4B). HCV RNA became undetectable in all three mice 1 week after the beginning of the therapy. After 4 weeks of treatment, one mouse died. In the remaining two mice, HCV RNA did not become positive after cessation of the therapy. One of the remaining two mice died at 20 weeks, and the remaining mouse was sacrificed at 24 weeks (12 weeks after the cessation of therapy). HCV was probably eliminated because no HCV RNA was detected by nested PCR in this mouse liver (Fig. 4C). As a control, HCV-infected mice were treated with 1500 IU/g/day of IFN-alpha alone for 4 weeks, resulting in a two log reduction (Fig. 4D). HCV RNA became undetectable with

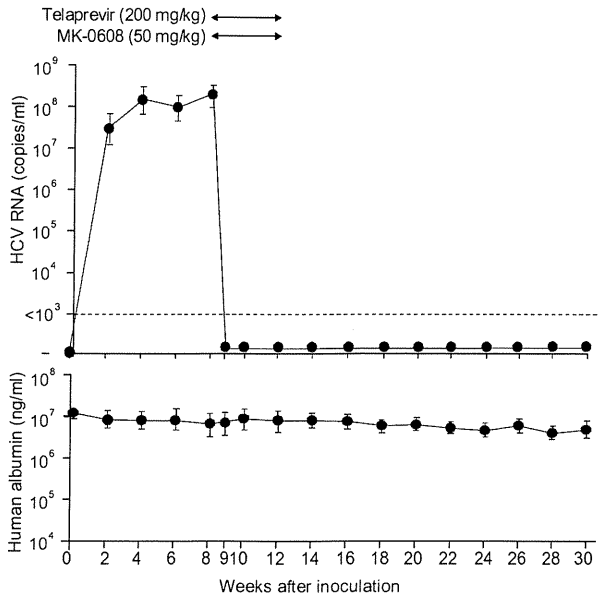

Fig. 5. High doses of MK-0608 and telaprevir combination treatment eliminates virus in HCV-infected mice. HCV-infected mice were treated with 50 mg/kg of MK-0608 and 200 mg/kg of telaprevir for 4 weeks. Mice serum samples were obtained at the indicated times, and HCV RNA titer (upper panel) and human serum albumin concentration (lower panel) were analyzed. Points represent the means ± SD of five mice.

administration of 7000 IU/g/day of IFN-alpha treatment. However, the virus rebounded after cessation of the therapy.

Four-week high dose combination therapy of MK-0608 and telaprevir eliminated HCV from mice

We investigated whether combination treatment with high doses of MK-0608 and telaprevir without IFN eliminates viruses from HCV-infected mice. Five HCV-infected mice were treated with high doses of MK-0608 (50 mg/kg) and telaprevir (200 mg/kg) for 4 weeks. Serum HCV RNA titer became undetectable 1 week after commencement of the therapy and remained undetectable in all mice at 30 weeks (18 weeks after cessation of the therapy) (Fig. 5). No apparent toxicity of the drugs was observed as none of the mice showed a decrease in the level of serum HSA.

Discussion

Since we began performing treatment experiments using human hepatocyte chimeric mice with HCV, we have administered many different drugs to analyze the effects on suppression or eradication of the virus. However, until we performed the experiments described in this study, we have never observed long term absence of the virus following cessation of the therapy [12,24]. Strikingly, after only 4 weeks of triple therapy with IFN, telaprevir and MK0608, was long term absence of the virus in mouse serum after cessation of the therapy visible (Fig. 4B). Furthermore, high dose telaprevir and MK-0608 combination therapy resulted in a similar absence of the virus for 16 weeks after cessation of therapy (Fig. 5). In this study, mice were treated with 200 mg/kg of telaprevir twice a day, and 1 week of the treatment resulted in an approximately 2 log reduction of HCV RNA (Fig. 3A), as has been observed previously in chronic hepatitis C patients treated with 450 mg of telaprevir every 8 hrs [25]. This result suggests that approximately 1/15th of a dose in this mouse model may be equivalent to a dose in humans.

During the observation period, some mice died. We do not think that this is due to the drug regimes because the chimeric mouse is weak, and approximately 50% of mice die spontaneously at week 6 after transplantation [26].

Sustained virological response, the complete elimination of the virus from the human body, is defined as testing negative for HCV RNA in serum for more than 24 weeks after cessation of the therapy. As the chimeric mouse used in this study is a weak animal, we were unable to monitor for absence of the virus beyond 24 weeks following cessation of therapy. However, negative testing for HCV RNA in mouse liver by nested PCR (Fig. 4C) 12 weeks after cessation of the therapy strongly suggests that HCV was completely eliminated from the mouse. Of course the mouse model differs from infection in humans where the virus replicates for years in the livers of infected patients. However, results of this study suggest that we will be able to eliminate the virus in humans by treating patients with regimens similar to those used in this study.

Until recently eradication of the virus with biochemical and histological improvement in chronically infected patients has long been reported only with the use of IFN or PEG-IFN [27,28]. Recently, Suzuki et al. reported for the first time eradication of the virus from chronically infected patients without IFN [29].

Elimination of the virus without IFN is desirable due to the many serious side effects of this drug [3,5–9]. However, emergence of drug resistance is a problem, as demonstrated in this study (Fig. 3) as well as in previous studies using replicon systems and HCV-infected chimpanzees [22,23]. A recent clinical study of NS3-4A and NS5B inhibitor combination therapy has reported that 13 days of this combination treatment achieved robust antiviral suppression in chronic hepatitis C patients [30]. As no study has tested the possibility of development of double drug resistant mutants, we will have to test if long term low dose treatment with any combination of STAT-C compounds might induce emergence of multi-drug resistant strains. Furthermore, as there is no report for emergence of IFN resistant strains, regimens such as combination therapy with multiple STAT-C drugs with a small or standard amount of IFN should be tested to develop the best therapy to eradicate the virus with a minimum of side effects and costs. Our further attempts to test possible combinations in mice to determine the best combination of STAT-C drugs will give us an insight into how to develop more effective therapeutic regimens in humans.

Financial support

This study was supported in part by a Grant-in-Aid for Scientific Research from the Japanese Ministry of Labor, Health and Welfare.

Conflict of interest

The authors who have taken part in this study declared that they do not have anything to disclose regarding conflict of interest with respect to this manuscript.

Research Article

Acknowledgments

The authors thank Rie Akiyama, Kazuyo Hattori, and Yoko Matsumoto for their expert technical help, and Dr. Naoya Sakamoto for providing Huh7/Rep-Neo cells.

References

[1] Niederau C, Lange S, Heintges T, Erhardt A, Buschkamp M, Hürter D, et al. Prognosis of chronic hepatitis C: results of a large, prospective cohort study. Hepatology 1998;28:1687–1695.

[2] Kiyosawa K, Sodeyama T, Tanaka E, Gibo Y, Yoshizawa K, Nakano Y, et al. Interrelationship of blood transfusion, non-A, non-B hepatitis and hepatocellular carcinoma: analysis by detection of antibody to hepatitis C virus. Hepatology 1990;12:671–675.

[3] Manns MP, McHutchison JG, Gordon SC, Rustgi VK, Shiffman M, Reindollar R, et al. Peginterferon alfa-2b plus ribavirin compared with interferon alfa-2b plus ribavirin for initial treatment of chronic hepatitis C: a randomised trial. Lancet 2001;358:958–965.

[4] Fried MW, Shiffman ML, Reddy KR, Smith C, Marinos G, Goncales Jr FL, et al. Peginterferon alfa-2a plus ribavirin for patients with chronic hepatitis C virus infection. N Engl J Med 2002;347:975–982.

[5] Hoofnagle JH, Ghany MG, Kleiner DE, Doo E, Heller T, Promart K, et al. Maintenance therapy with ribavirin in patients with chronic hepatitis C who fail to respond to combination therapy with interferon alfa and ribavirin. Hepatology 2003;38:66–74.

[6] Schinazi RF, Bassit L, Gavegnano C. HCV drug discovery aimed at viral eradication. J Viral Hepat 2010;17:77–90.

[7] Lin C, Gates CA, Rao BG, Brennan DL, Fulghum JR, Luong YP, et al. In vitro studies of cross-resistance mutations against two hepatitis C virus serine protease inhibitors, VX-950 and BILN 2061. J Biol Chem 2005;280: 36784–36791.

[8] Mo H, Lu L, Pilot-Matias T, Pithawalla R, Mondal R, Masse S, et al. Mutations conferring resistance to a hepatitis C virus (HCV) RNA-dependent RNA polymerase inhibitor alone or in combination with an HCV serine protease inhibitor in vitro. Antimicrob Agents Chemother 2005;49:4305–4314.

[9] Björnsson E, Verbaan H, Oksanen A, Frydén A, Johansson J, Friberg S, et al. Health-related quality of life in patients with different stages of liver disease induced by hepatitis C. Scand J Gastroenterol 2009;44:878–887.

[10] Mercer DF, Schiller DE, Elliott JF, Douglas DN, Hao C, Rinfret A, et al. Hepatitis C virus replication in mice with chimeric human livers. Nat Med 2001;7:927–933.

[11] Kneteman NM, Weiner AJ, O'Connell J, Collett M, Gao T, Aukerman L, et al. Anti-HCV therapies in chimeric scid-Alb/uPA mice parallel outcomes in human clinical application. Hepatology 2006;43:1346–1353.

[12] Hiraga N, Imamura M, Tsuge M, Noguchi C, Takahashi S, Iwao E, et al. Infection of human hepatocyte chimeric mouse with genetically engineered hepatitis C virus and its susceptibility to interferon. FEBS Lett 2007;581: 1983–1987.

[13] Kimura T, Imamura M, Hiraga N, Hatakeyama T, Miki D, Noguchi C, et al. Establishment of an infectious genotype 1b hepatitis C virus clone in human hepatocyte chimeric mice. J Gen Virol 2008;89:2108–2113.

[14] Kamiya N, Iwao E, Hiraga N, Tsuge M, Imamura M, Takahashi S, et al. Practical evaluation of a mouse with chimeric human liver model for hepatitis C virus infection using an NS3-4A protease inhibitor. J Gen Virol 2010;91:1668–1677.

[15] Lin C, Kwong AD, Perni RB. Discovery and development of VX-950, a novel, covalent, and reversible inhibitor of hepatitis C virus NS3.4A serine protease. Infect Disord Drug Targets 2006;6:3–16.

[16] Migliaccio G, Tomassini JE, Carroll SS, Tomei L, Altamura S, Bhat B, et al. Characterization of resistance to non-obligate chain-terminating ribonucleoside analogs that inhibit hepatitis C virus replication in vitro. J Biol Chem 2003;278:49164–49170.

[17] Guo JT, Bichko VV, Seeger C. Effect of alpha interferon on hepatitis C virus replicon. J Virol 2001;75:8516–8523.

[18] Tanabe Y, Sakamoto N, Enomoto N, Kurosaki M, Ueda E, Maekawa S, et al. Synergistic inhibition of intracellular hepatitis C virus replication by combination of ribavirin and interferon-alpha. J Infect Dis 2004;189: 1129–1139.

[19] Yokota T, Sakamoto N, Enomoto N, Tanabe Y, Miyagishi M, Maekawa S, et al. Inhibition of intracellular hepatitis C virus replication by synthetic and vector-derived small interfering RNAs. EMBO Rep 2003;4:602–608.

[20] Tateno C, Yoshizane Y, Saito N, Kataoka M, Utoh R, Yamasaki C, et al. Near completely humanized liver in mice shows human-type metabolic response to drugs. Am J Pathol 2004;165:901–912.

[21] Tsuge M, Hiraga N, Takaishi H, Noguchi C, Oga H, Imamura M, et al. Infection of human hepatocyte chimeric mouse with genetically engineered hepatitis B virus. Hepatology 2005;42:1046–1054.

[22] Kieffer TL, Kwong AD, Picchio GR. Viral resistance to specifically targeted antiviral therapies for hepatitis C (STAT-Cs). J Antimicrob Chemother 2010;65:202–212.

[23] Carroll SS, Ludmerer S, Handt L, Koeplinger K, Zhang NR, Graham D. Robust antiviral efficacy upon administration of a nucleoside analog to hepatitis C virus-infected chimpanzees. Antimicrob Agents Chemother 2009;53: 926–934.

[24] Matsumura T, Hu Z, Kato T, Dreux M, Zhang YY, Imamura M, et al. Amphipathic DNA polymers inhibit hepatitis C virus infection by blocking viral entry. Gastroenterology 2009;137:673–681.

[25] Reesink HW, Zeuzem S, Weegink CJ, Forestier N, van Vliet A, de Rooji J, et al. Rapid decline of viral RNA in hepatitis C patients treated with VX-950: a phase Ib, placebo-controlled, randomized study. Gastroenterology 2006;131:997–1002.

[26] Vanwolleghem T, Libbrecht L, Hansen BE, Desombere I, Roskams T, Meuleman P, et al. Factors determining successful engrafment of hepatocytes and susceptibility to hepatitis B and C virus infection in uPA-SCID mice. J Hepatol 2010;53:468–476.

[27] Chayama K, Saitoh S, Arase Y, Ikeda K, Matsumoto T, Sakai Y, et al. Effect of interferon administration on serum hepatitis C virus RNA in patients with chronic hepatitis C. Hepatology 1991;13:1040–1043.

[28] Poynard T, McHutchison J, Manns M, Trepo C, Lindsay K, Goodman Z, et al. Impact of pegylated interferon alfa-2b and ribavirin on liver fibrosis in patients with chronic hepatitis C. Gastroenterology 2002;122:1303–1313.

[29] Suzuki F, Suzuki Y, Akuta N, Sezaki H, Yatsuji H, Arase Y, et al. Sustained virological response in a patient with chronic hepatitis C treated by monotherapy with the NS3-4A protease inhibitor telaprevir. J Clin Virol 2010;47:76–78.

[30] Gane E, Roberts S, Stedman C, Angus P, Ritchie B, Elston R, et al. 749 Early on-treatment responses during pegylated IFN plus rivavirin are increased following 13 days of combination nucleoside polymerase (RG7128) and protease (RG7227) inhibitor therapy (INFORM-1). J Hepatol 2010;51: S291–S292.

Supplemental Material can be found at:
http://dmd.aspetjournals.org/content/suppl/2011/11/02/dmd.111.040923.DC1.html

1521-009X/12/4002-322–328$25.00
DRUG METABOLISM AND DISPOSITION
Copyright © 2012 by The American Society for Pharmacology and Experimental Therapeutics
DMD 40:322–328, 2012

Vol. 40, No. 2
40923/3743170

Prediction of In Vivo Hepatic Clearance and Half-Life of Drug Candidates in Human Using Chimeric Mice with Humanized Liver[S]

Seigo Sanoh, Aya Horiguchi, Kazumi Sugihara, Yaichiro Kotake, Yoshitaka Tayama, Hiroki Ohshita, Chise Tateno, Toru Horie, Shigeyuki Kitamura, and Shigeru Ohta

Graduate School of Biomedical Sciences (S.S., A.H., Y.K., S.O.) and Liver Research Project Center, Hiroshima University, Hiroshima, Japan (C.T.); Faculty of Pharmaceutical Sciences, Hiroshima International University, Hiroshima, Japan (K.S., Y.T.); PXB Mouse Production Department (H.O.) and R&D Department (C.T.), PhoenixBio Co., Ltd., Hiroshima, Japan; DeThree Research Laboratories, Ibaraki, Japan (T.H.); and Nihon Pharmaceutical University, Saitama, Japan (S.K.)

Received August 5, 2011; accepted November 2, 2011

ABSTRACT:

Accurate prediction of pharmacokinetics (PK) parameters in humans from animal data is difficult for various reasons, including species differences. However, chimeric mice with humanized liver (PXB mice; urokinase-type plasminogen activator/severe combined immunodeficiency mice repopulated with approximately 80% human hepatocytes) have been developed. The expression levels and metabolic activities of cytochrome P450 (P450) and non-P450 enzymes in the livers of PXB mice are similar to those in humans. In this study, we examined the predictability for human PK parameters from data obtained in PXB mice. Elimination of selected drugs involves multiple metabolic pathways mediated not only by P450 but also by non-P450 enzymes, such as UDP-glucuronosyltransferase, sulfotransferase, and aldehyde oxidase in liver. Direct comparison between in vitro intrinsic clearance ($CL_{int,in\ vitro}$) in PXB mice hepatocytes and in vivo intrinsic clearance ($CL_{int,in\ vivo}$) in humans, calculated based on a well stirred model, showed a moderate correlation ($r^2 = 0.475$, $p = 0.009$). However, when $CL_{int,in\ vivo}$ values in humans and PXB mice were compared similarly, there was a good correlation ($r^2 = 0.754$, $p = 1.174 \times 10^{-4}$). Elimination half-life ($t_{1/2}$) after intravenous administration also showed a good correlation ($r^2 = 0.886$, $p = 1.506 \times 10^{-4}$) between humans and PXB mice. The rank order of CL and $t_{1/2}$ in human could be predicted at least, although it may not be possible to predict absolute values due to rather large prediction errors. Our results indicate that in vitro and in vivo experiments with PXB mice should be useful at least for semiquantitative prediction of the PK characteristics of candidate drugs in humans.

Introduction

It is important to predict human pharmacokinetics (PK) and metabolism of drug candidates in the preclinical stage of pharmaceutical development. Various approaches to predict human clearance (CL) with in vitro metabolic systems, such as human liver microsomes and hepatocytes, have been reported (Nagilla et al., 2006; Brown et al., 2007; Fagerholm, 2007; Stringer et al., 2008; Chiba et al., 2009; Hallifax et al., 2010) but with limited success. One of the reasons for the discrepancy between predicted and observed CL may be that the preparation, storage, and experimental treatment of hepatocytes alter the normal function of metabolic enzymes (Wang et al., 2005). Although this might be ameliorated by using fresh hepatocytes immediately after isolation from the liver, these are not readily available and in any case show considerable interindividual differences.

It has become possible recently to predict CL and half-life ($t_{1/2}$) by means of computational approaches and physiologically based modeling (Ekins and Obach, 2000; De Buck et al., 2007; Tabata et al., 2009; Paixão et al., 2010). Accurate prediction of human PK is a key issue for the development of new drugs, because many new drug candidates with diverse chemical structures are metabolized not only by cytochrome P450 (P450) but also by non-P450 enzymes, such as UDP-glucuronosyltransferase (UGT) and sulfotransferase (SULT). It is also necessary to take into account the effects of cell permeability, transporter-mediated uptake, and excretion (Chiba et al., 2009; Huang et al., 2010).

Chimeric mice with humanized liver (PXB mice; PhoenixBio Co., Ltd., Hiroshima, Japan) have been generated from urokinase-type plasminogen activator/severe combined immunodeficiency mice transplanted with human hepatocytes (Tateno et al., 2004). In these mice, approximately 80% of the hepatocytes are human. The expression levels and metabolic activities of P450 and non-P450 enzymes in

This work was supported by a Grant-in-Aid for Young Scientists (B) from Japan Society for the Promotion of Science [Grant 22790109]; and PhoenixBio, Co., Ltd.

Article, publication date, and citation information can be found at http://dmd.aspetjournals.org.

http://dx.doi.org/10.1124/dmd.111.040923.

[S] The online version of this article (available at http://dmd.aspetjournals.org) contains supplemental material.

ABBREVIATIONS: PK, pharmacokinetics; CL, clearance; AO, aldehyde oxidase; $CL_{int,in\ vitro}$, in vitro intrinsic clearance; $CL_{int,in\ vivo}$, in vitro intrinsic clearance; CL_{oral}, oral clearance; CL_t, total clearance; P450, cytochrome P450; DMSO, dimethyl sulfoxide; fu, plasma unbound fraction; h-hepatocytes, PXB mice hepatocytes; LC/MS/MS, liquid chromatography tandem mass spectrometry; NAT, *N*-acetyltransferase; PXB mice, chimeric mice with humanized liver; *Q*, hepatic blood flow; Rb, blood/plasma concentration ratio; RI, replacement index; SULT, sulfotransferase; $t_{1/2}$, half-life; UGT, UDP-glucuronosyltransferase; AUC_{iv}, area under the concentration versus time curve by intravenous administration.

DMD DRUG METABOLISM AND DISPOSITION aspet

livers of PXB mice with a high replacement index (RI) are similar to those of humans (Katoh et al., 2004, 2005), and human-specific metabolites are formed in PXB mice (Inoue et al., 2009; Kamimura et al., 2010; Yamazaki et al., 2010; De Serres et al., 2011). Thus, PXB mice could be a good in vivo model for predicting drug metabolism in humans.

However, quantitative methods for predicting PK parameters of humans from data in PXB mice have not been established yet. Therefore, we selected 13 model compounds that are metabolized by P450 and/or non-P450 enzymes in liver and compared the PK parameters in humans and PXB mice, using both in vitro and in vivo approaches, to evaluate the utility of this animal model for the prediction of human PK.

Materials and Methods

Chemicals. 6-Deoxypenciclovir and mirtazapine were obtained from Toronto Research Chemicals Inc. (North York, ON, Canada). Dapsone, lamotrigine, salbutamol, and sulindac were purchased from Sigma-Aldrich (St. Louis, MO). Diclofenac was purchased from Tokyo Chemical Industry Co. Ltd. (Tokyo, Japan). Fasudil was obtained from Tocris Bioscience (Bristol, UK). (*S*)-Naproxen was purchased from Cayman Chemical (Ann Arbor, MI). Ibuprofen, ketoprofen, and (*S*)-warfarin were purchased from Wako Pure Chemicals (Osaka, Japan). Zaleplon was kindly provided by King Pharm. Inc. (Bristol, UK). All of the other regents and solvents were commercial products of the highest available grade or analytical grade.

Animals. The present study was approved by the animal ethics committee and was conducted in accordance with the regulations on the use of living modified organisms of Hiroshima University. PXB mice (10–14 weeks of age) with human hepatocytes were prepared by the reported method (Tateno et al., 2004). Human hepatocytes of a donor (African-American boy, 5 years old) were obtained from BD Biosciences (San Jose, CA). PXB mice were housed in a temperature- and humidity-controlled environment under a 12-h light/dark cycle.

The RI was determined by the measurement of human albumin in blood collected from the tail vein. The RI was estimated by the correlation curve between the human albumin levels in mouse blood and determined by using human-specific cytokeratin 8/18-immunostained liver sections (Tateno et al., 2004). The RI values of PXB mice used in this study ranged from 73.4 to 93.4%.

Administration. Drug solution (5 ml/kg) was administered intravenously to PXB mice at 0.3 to 5 mg/kg body weight. Solutions of dapsone, diclofenac, 6-deoxypenciclovir, fasudil, ketoprofen, ibuprofen, mirtazapine, naproxen, salbutamol, and sulindac were prepared in saline. In the cases of ketoprofen, ibuprofen, naproxen, and sulindac, equivalent amounts of alkali were added. Dapsone solutions contained 10% dimethyl sulfoxide (DMSO), and mirtazapine solutions were prepared with 10% DMSO and equivalent amounts of hydrochloric acid. Lamotrigine, and zaleplon solutions were prepared with 10% DMSO and 10% polyethylene glycol 400 in saline. Equivalent amounts of hydrochloric acid also were added to the solutions of lamotrigine and zaleplon. Warfarin was formulated in 3% DMSO and 97% saline with an equivalent amount of sodium hydroxide.

Blood samples after dosing were collected from orbital veins of PXB mice at predetermined times using heparinized glass. These samples were centrifuged, and the plasma was stored at −30°C.

Determination of Drug Concentrations in Plasma. A 10 μl aliquot of plasma was added to 40 μl of acetonitrile or methanol containing an internal standard (carbamazepine, ketoprofen, or ibuprofen). The mixtures were centrifuged at 14,000*g* for 5 min, and the supernatant was subjected to liquid chromatography tandem mass spectrometry (LC/MS/MS).

Isolation and Purification of Hepatocytes from PXB Mice. Fresh hepatocytes were isolated from PXB mice (13–15 weeks of age) by means of the in situ collagenase perfusion method and purified as described previously (Yamasaki et al., 2010). PXB mouse hepatocytes (h-hepatocytes) contained approximately 7% mouse hepatocytes. We used h-hepatocytes purified by the use of 66Z rat IgG and magnetic beads bearing anti-rat IgG antibodies. The magnetic removal of mouse hepatocytes reduced the level of mouse hepatocytes to approximately 2% (in this study, the purity of human hepatocytes from PXB mouse hepatocytes ranged from 96.6 to 99.7% after purification). Cell viability of the hepatocytes used in the experiments ranged from 79 to 91%, as determined by means of the trypan blue exclusion test.

In Vitro Metabolic Studies Using h-Hepatocytes. The h-hepatocyte suspension (1×10^6 cells/ml) was incubated in Krebs-Henseleit buffer without serum in the presence of 10 μM of the test drug at 37°C under an atmosphere of 5% CO_2/95% O_2. The final concentration of acetonitrile was 0.5% (v/v) in the reaction mixture. The plates (24 wells) were shaken gently with an orbital shaker. The incubation mixture was sampled at 0, 0.25, 0.5, 1, and 2 h after treatment, and reactions were stopped by freezing the mixture in liquid nitrogen. When required, the samples were thawed, spiked with two volumes of acetonitrile or methanol containing an internal standard, and centrifuged. Aliquots of the supernatants were subjected to LC/MS/MS.

LC/MS/MS Conditions. Aliquots (10 μl) of plasma and h-hepatocyte suspension were introduced into the high-performance liquid chromatography system with an autosampler (Agilent Technologies, Santa Clara, CA). Several mobile phase conditions were used. Mobile phase condition 1 consisted of 10 mM ammonium acetate (A) and acetonitrile (B) on an Inertsil ODS-3 column (3 μm, 50 × 2.1 mm; GL Sciences Inc., Tokyo, Japan) at 40°C for the analysis of diclofenac, ibuprofen, ketoprofen, mirtazapine, (*S*)-naproxen, sulindac, and (*S*)-warfarin. The flow rate was set at 0.2 ml/min. The starting condition for the high-performance liquid chromatography gradient was 90:10 (A/B). From 0 to 5 min, the mobile phase composition was changed linearly to 10:90 (A/B), and this was held until 8 min. The gradient then was returned to 90:10 (A/B)

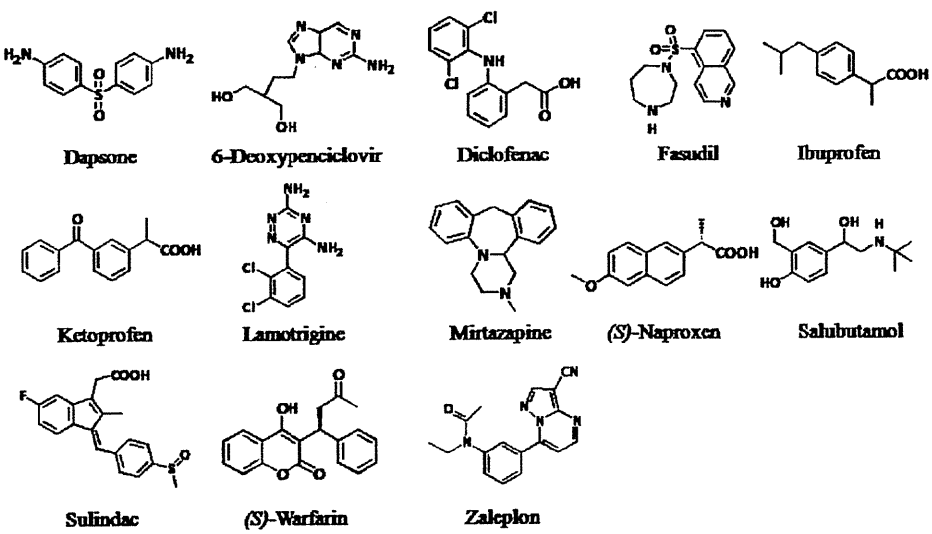

FIG. 1. Chemical structures of the model compounds used in this study.

DMD DRUG METABOLISM AND DISPOSITION aspet

TABLE 1

Literature values of plasma clearance, half-life, unbound fraction in plasma, blood/plasma concentration ratio, and metabolic enzymes in humans for the model compounds examined in this analysis

Rb values of fasudil, lamotrigine, and sulindac were assumed to be 1 due to unavailable data from the literature. References are in Supplemental Tables 1 and 2

Compounds	CL_t or CL_{oral}	$t_{1/2}$	fu	Rb	Metabolic Enzymes
	ml · min^{-1} · *kg*$^{-1}$	*h*			
Dapsone	0.48	22	0.25	1.04	CYP2C9, CYP3A4, NAT
6-Deoxypenciclovir[a,c]	118	–	1	1.2	AO
Diclofenac	3.5	1.4	0.005	0.55	CYP2C9, UGT2B7, UGT1A9
Fasudil	73.2	0.26	0.51	1	AO
Ibuprofen	0.82	1.6	0.006	0.55	CYP2C9, UGT2B7
Ketoprofen	1.6	2.1	0.008	0.55	UGT2B7
Lamotrigine[a]	0.3	–	0.45	1	UGT1A4, UGT2B7
Mirtazapine	8.0	15	0.15	0.67	CYP1A2, CYP2D6, CYP3A4
(*S*)-Naproxen	0.1	–	0.01	0.55	CYP2C9, CYP1A2, UGT2B7
Salbutamol	7.7	3.9	0.925	0.96	SULT1A3
Sulindac[a]	3.3	–	0.069	1	AO
(*S*)-Warfarin	0.055	29	0.015	0.55	CYP2C9
Zaleplon	16	1.1	0.4	0.99	AO, CYP3A4

[a] From oral administration data.
[c] Calculated as famciclovir, which is prodrug of 6-deoxypenciclovir.
–, Unavailable data from intravenous administration.

linearly from 8 to 8.1 min, and the column was re-equilibrated to the initial condition.

Mobile phase condition 2 consisted of 0.1% formic acid (A) and methanol (B) on a YMC-Triart C18 column (3 μm, 50 × 2.1 mm; YMC Co., Ltd., Kyoto, Japan) for the analysis of dapsone, 6-deoxypenciclovir, fasudil, lamotrigine, salbutamol, and zaleplon. The starting condition was 90:10 (A/B). From 0 to 5 min, the mobile phase composition was changed linearly to 10:90 (A/B), and this was maintained until 8 min, then the column was re-equilibrated to the initial condition.

The MS/MS experiments were conducted by using API2000 LC/MS/MS systems (Applied Biosystems, Foster, CA). Mass number of the ionization mode, molecular ion, and product ion for the model compounds were as follows: dapsone *m/z* = 248.99 $[M + H]^+$ to 92.18, 6-deoxypenciclovir *m/z* = 238.05 $[M + H]^+$ to 210.95, diclofenac *m/z* = 294.14 $[M + H]^+$ to 249.53, fasudil *m/z* = 292.07 $[M + H]^+$ to 99.09, ibuprofen *m/z* = 204.88 $[M + H]^+$ to 158.52, ketoprofen *m/z* = 253.16 $[M + H]^+$ to 208.73, lamotrigine *m/z* = 256.03 $[M + H]^+$ to 210.96 mirtazapine *m/z* = 266.14 $[M + H]^+$ to 194.97, (*S*)-naproxen *m/z* = 228.68 $[M + H]^+$ to 168.55, salbutamol *m/z* = 240.18 $[M + H]^+$ to148.03, sulindac *m/z* = 357.07 $[M + H]^+$ to 232.96, (*S*)-warfarin *m/z* = 309.06 $[M + H]^+$ to162.97, zaleplon *m/z* = 306.08 $[M + H]^+$ to 236.12.

Determination of PK Parameters. Pharmacokinetic parameters were determined by noncompartmental methods using the concentration-time curve profile. The total clearances (CL_t) after intravenous administration were calculated as dose/AUC_{∞}. AUC_{∞} values were estimated from the time course using the trapezoidal method with extrapolation from the last quantifiable point to infinity. The terminal elimination $t_{1/2}$ was estimated as ln 2/*ke*, where *ke* is that of the plot of the terminal elimination phase on a logarithmic scale.

Calculation of In Vitro Intrinsic Clearance. In vitro intrinsic clearance ($CL_{int,in\ vitro}$) was calculated from the time course of the disappearance of the test drug during incubation with h-hepatocytes. Each plot was fitted to the first-order elimination rate constant as $C(t) = C_0 \cdot \exp(-ke \cdot t)$, where $C(t)$ and C_0 are the concentration of unchanged test drug at incubation time *t* and that at preincubation and *ke* is the disappearance rate constant of the unchanged drug.

Subsequently, $CL_{int,in\ vitro}$ (μl · min^{-1} · 10^6 cells^{-1}) values were converted to $CL_{int,in\ vitro}$ (ml · min^{-1} · kg^{-1}) for the whole body. $CL_{int,in\ vitro}$ data were scaled up using physiological parameters, human liver weight 26 g/kg (Davies and Morris, 1993) and PXB mouse liver weight 140 g/kg, and the hepatocellularity (132 × 10^6 cells/g liver) of PXB mice. These parameters were taken from the average of observed data in PXB mice (RI = 80%).

Calculation of In Vivo Intrinsic Clearance. CL_t of PXB mice was calculated from the plasma concentrations after dosing using noncompartmental methods as described. CL_t was assumed to be equal to the hepatic clearance.

Values of CL_t, plasma unbound fraction (fu), and blood/plasma concentration ratio (Rb) in humans were taken from the literature.

In vivo intrinsic clearance ($CL_{int,in\ vivo}$) was calculated from the in vivo CL_t, fu, Rb, and average hepatic blood flow (Q) based on a well stirred model as $CL_{int,in\ vivo} = CL_t/\{(fu/Rb) \times (1 - CL_t/Q)\}$ (Pang and Rowland, 1977). These CL_t values were converted to blood clearance using Rb values.

The Q values of humans and PXB mice were set at 21 and 90 ml · min^{-1} · kg^{-1} (same as in normal mice), respectively (Davies and Morris, 1993). In addition, Rb and fu of human were assumed to be equivalent to those of PXB mice. If CL_t of drugs exceeded liver blood flow, then the hepatic clearance was taken as 90% of liver blood flow. $CL_{int,in\ vivo}$ of 6-deoxypenciclovir, lamotrigine, and sulindac were evaluated from oral clearance (CL_{oral}) as CL_{oral}/fu/Rb.

Results

Selection of the Model Compounds for Analysis. In this study, we selected 13 compounds with diverse chemical structures (Fig. 1). Elimination of these selected drugs involves multiple metabolic pathways mediated not only by P450 but also by non-P450 enzymes, such as UGT, SULT, and aldehyde oxidase (AO) in liver. Mirtazapine and warfarin were known to be mainly metabolized by P450. Diclofenac, ibuprofen, and naproxen were metabolized by both UGT and P450. Furthermore, the model compounds metabolized by AO, such as

TABLE 2

Estimation of $CL_{int,in\ vitro}$ (μl · min^{-1} · 10^6 cells^{-1}) in PXB mice hepatocytes and scaling to humans and PXB mice

$CL_{int,in\ vitro}$ (μl · min^{-1} · 10^6 cells^{-1}) values were converted to $CL_{int,in\ vitro}$ (ml · min^{-1} · kg^{-1}) for the whole body. $CL_{int,in\ vitro}$ data were scaled up using physiological parameters, human liver weight (26 g/kg) and PXB mouse liver weight (140 g/kg), and the hepatocellularity (132 × 10^6 cells/g liver) of PXB mice. Each value represents the mean ± S.D. (n = 3)

Compounds	$CL_{int,in\ vitro}$	Scaled $CL_{int,in\ vitro}$ (Human)	Scaled $CL_{int,in\ vitro}$ (PXB Mice)
	μl · min^{-1} · *10*^{6} *cells*$^{-1}$	*ml · min*$^{-1}$ · *kg*$^{-1}$	
Dapsone	2.3 ± 1.2	8.0 ± 4.0	43.1 ± 21.3
6-Deoxypenciclovir	5.3 ± 1.2	18.3 ± 4.2	98.6 ± 22.4
Diclofenac	24.7 ± 1.2	84.7 ± 4.0	455.8 ± 21.3
Fasudil	35.7 ± 13.3	122.4 ± 45.6	659.1 ± 245.4
Ibuprofen	13.3 ± 2.1	45.8 ± 7.1	246.4 ± 38.5
Ketoprofen	6.0 ± 1.0	20.6 ± 3.4	110.9 ± 18.5
Lamotrigine	1.4 ± 1.0	4.8 ± 3.6	25.9 ± 19.2
Mirtazapine	6.3 ± 1.2	21.7 ± 4.0	117.0 ± 21.3
(*S*)-Naproxen	12.7 ± 2.5	43.5 ± 8.6	234.1 ± 46.5
Salbutamol	1.0 ± 1.0	3.3 ± 3.3	17.9 ± 17.8
Sulindac	2.0 ± 2.0	7.0 ± 6.7	37.6 ± 36.0
(*S*)-Warfarin	1.2 ± 0.7	4.1 ± 2.5	22.2 ± 13.3
Zaleplon	2.3 ± 1.2	8.0 ± 4.0	43.1 ± 21.3

DMD DRUG METABOLISM AND DISPOSITION aspet

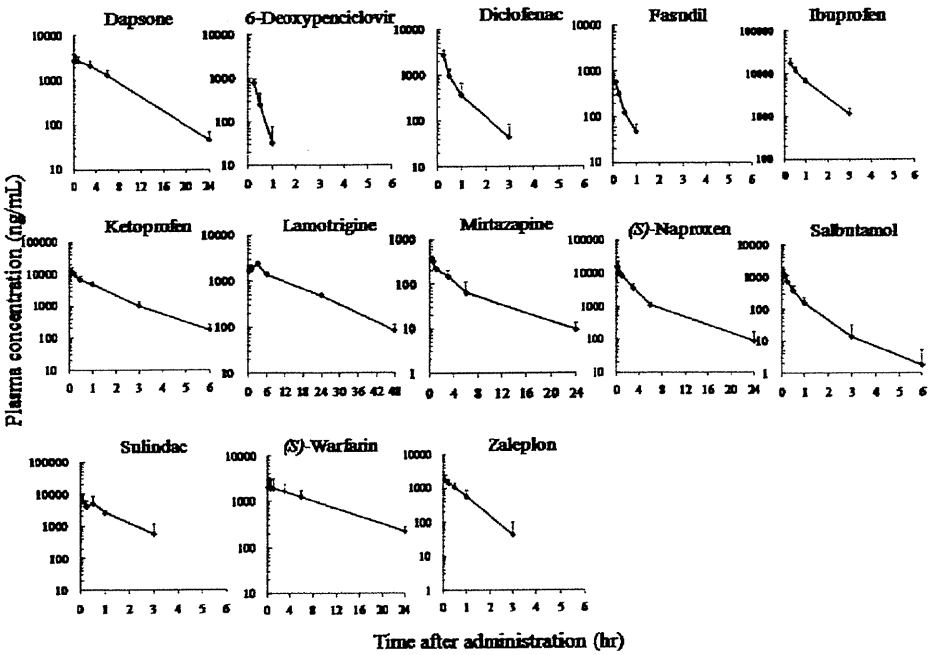

FIG. 2. Plasma concentrations after intravenous administration to PXB mice. Each point represents the mean + S.D. (n = 3–5).

6-deoxypenciclovir, fasudil, sulindac, and zaleplon, were added in this study. These were reflected in the data set that spanned a wide range of PK parameter characteristics. CL_t and $t_{1/2}$ after intravenous administration of selected model drugs to humans were obtained from the literature. If CL_t after intravenous administration was not available from the literature, we used the value of CL_t/F after oral administration. The PK parameters and the major enzymes responsible for drug metabolism in humans are shown in Table 1. The spreadsheet containing these values with the literature references is included as an attachment in the supplemental data (Supplemental Tables 1 and 2).

Disappearance of Parent Drugs after Incubation. Remaining amounts of all of the compounds decreased linearly fo r 2 h on incubation with h-hepatocytes. The values of $CL_{int,in\ vitro}$ in hepatocytes, calculated using scaling factors to humans and PXB mice whole body as described under *Materials and Methods*, are listed in Table 2. These $CL_{int,in\ vitro}$ values covered a wide range. Fasudil showed high clearance, whereas warfarin was very stable.

PK Study of the Model Compounds in PXB Mice. Plasma concentrations and PK parameters in PXB mice after intravenous administration of drug solutions at 0.3 to 5 mg/kg are shown in Fig. 2 and Tables 3 and 4. Each RI value in PXB mice was 73.4 to 93.4%.

CL_t values of warfarin and lamotrigine were relatively low, whereas those of fasudil and salbutamol were much higher: the range of CL_t was 0.2 to 198 ml · min^{-1} · kg^{-1}. The $t_{1/2}$ value of lamotrigine was the longest, and those of 6-deoxypenciclovir and fasudil were short, as shown in Table 3.

Comparison of Intrinsic CL between h-Hepatocytes and Humans. Direct comparison between $CL_{int,in\ vitro}$ from h-hepatocytes and $CL_{int,in\ vivo}$ calculated for a well stirred model in humans showed a moderate correlation (r^2 = 0.475, p = 0.009) (Fig. 3). For 2 of 13 (15%) compounds, observed $CL_{int,in\ vivo}$ was predicted within a 3-fold error from hepatocyte $CL_{int,in\ vitro}$. However, for 8 of 13 (62%) compounds, observed $CL_{int,in\ vivo}$ was predicted with a 3- to 10-fold error.

Figure 4 shows the relationship between $CL_{int,in\ vivo}$ and $CL_{int,in\ vitro}$ for PXB mice: again, the correlation was moderate (r^2 = 0.435, p =

TABLE 3

Experimental conditions and RI values in PXB mice used for PK study

Each compound was administered intravenously to PXB mice at 0.3 to 5 mg/kg body weight. The values of RI of PXB mice ranged from 73.4 to 93.4%. Each value represents the mean ± S.D. (n = 3–5)

Compounds	Dose	RI	CL_t	$t_{1/2}$
	mg/kg	%	ml · min^{-1} · kg^{-1}	h
Dapsone	3.0	77.4 ± 5.5	2.1 ± 0.5	4.5 ± 1.1
6-Deoxypenciclovir	3.0	93.4 ± 4.2	71.2 ± 13.0	0.1 ± 0.1
Diclofenac	3.0	76.4 ± 2.1	16.4 ± 4.3	0.6 ± 0.2
Fasudil	3.0	75.8 ± 1.3	198.1 ± 14.6	0.3 ± 0.1
Ibuprofen	5.0	73.4 ± 3.2	3.8 ± 1.0	0.7 ± 0.1
Ketoprofen	3.0	74.0 ± 1.1	3.3 ± 0.6	1.1 ± 0.1
Lamotrigine	3.0	77.1 ± 4.0	1.4 ± 0.2	10.1 ± 0.9
Mirtazapine	3.0	79.8 ± 1.7	30.4 ± 9.4	6.0 ± 1.4
(*S*)-Naproxen	5.0	82.2 ± 6.1	2.2 ± 0.5	4.8 ± 2.7
Salbutamol	3.0	74.5 ± 0.7	79.9 ± 34.0	0.6 ± 0.3
Sulindac	3.0	74.5 ± 2.0	5.6 ± 1.3	1.2 ± 0.8
(*S*)-Warfarin	0.3	75.3 ± 1.8	0.2 ± 0.1	8.2 ± 2.8
Zaleplon	3.0	77.1 ± 3.7	48.1 ± 7.1	0.7 ± 0.4

TABLE 4

$CL_{int,in\ vivo}$ of humans and PXB mice, calculated by a well stirred model

$CL_{int,in\ vivo}$ was calculated from in vivo CL_t, fu, Rb, and Q based on a well stirred model. The Q values of humans and PXB mice were set at 21 and 90 ml · min^{-1} · kg^{-1} (same as in normal mice), respectively. In addition, Rb and fu of human were assumed to be equivalent to those of PXB mice. If total CL of drugs exceeded liver blood flow, then the hepatic clearance was taken as 90% of liver blood flow. $CL_{int,in\ vivo}$ of 6-deoxypenciclovir, lamotrigine, and sulindac were evaluated from $CL_{s,t}$ as $CL_{s,t}$/fu/Rb.

Compounds	Human $CL_{int,in\ vivo}$	PXB Mice $CL_{int,in\ vivo}$
	ml · min^{-1} · kg^{-1}	
Dapsone	2.0	8.6
6-Deoxypenciclovir	118.0	209.0
Diclofenac	1004.3	4905.1
Fasudil	370.6	1588.2
Ibuprofen	147.1	686.0
Ketoprofen	232.2	442.0
Lamotrigine	0.7	3.2
Mirtazapine	123.6	408.7
(*S*)-Naproxen	10.1	230.2
Salbutamol	13.5	1148.2
Sulindac	47.8	86.5
(*S*)-Warfarin	3.7	13.4
Zaleplon	173.6	261.3

DRUG METABOLISM AND DISPOSITION DMD aspet

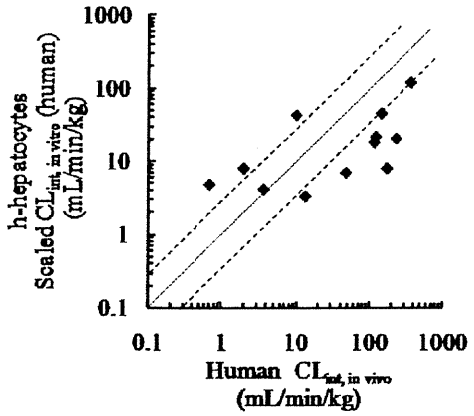

FIG. 3. Correlation between observed human $CL_{int,in\ vivo}$ and $CL_{int,in\ vivo}$ of PXB mouse hepatocytes, calculated as described in the text. The solid line represents unity. The dotted line represents the range within 3-fold of unity.

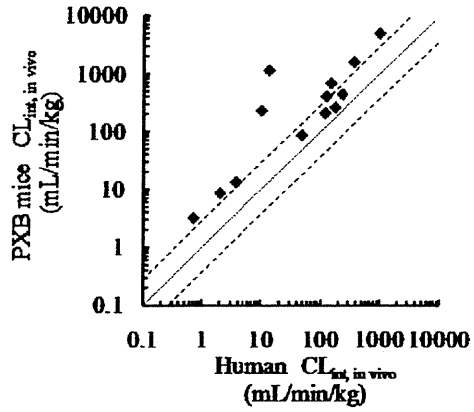

FIG. 5. Correlation of $CL_{int,in\ vivo}$ between humans and PXB mice, calculated as described in the text. The solid line represents unity. The dotted line represents the range within 3-fold of unity.

0.014). For 6 of 13 (46%) compounds, $CL_{int,in\ vivo}$ of PXB mice was predicted within a 3-fold error from h-hepatocyte $CL_{int,in\ vitro}$. For 5 of 13 (38%) compounds, $CL_{int,in\ vivo}$ was predicted within a 3- to 10-fold error.

Relationship between Intrinsic Clearance in Humans and PXB Mice In Vivo. We directly compared $CL_{int,in\ vivo}$ calculated based on a well stirred model in humans and PXB mice. As shown in Fig. 5, there was a good correlation ($r^2 = 0.754$, $p = 1.174 \times 10^{-4}$) between literature $CL_{int,in\ vivo}$ in human and measured $CL_{int,in\ vivo}$ of PXB mice for these compounds. For 4 of 13 (31%) compounds, observed $CL_{int,in\ vivo}$ in humans was predicted within a 3-fold error from PXB mouse $CL_{int,in\ vivo}$. For 7 of 13 (54%) compounds, human $CL_{int,in\ vivo}$ was predicted within a 3- to 10-fold error.

Relationship of Elimination $t_{1/2}$ between Humans and PXB mice. Figure 6 shows the relationship of $t_{1/2}$ after intravenous administration between humans and PXB mice. Compounds for which literature data were not available were excluded from this figure. A good correlation ($r^2 = 0.886$, $p = 1.506 \times 10^{-4}$) was found. For 6 of 9 (67%) compounds, human observed $t_{1/2}$ was predicted within a 3-fold error from PXB mice $t_{1/2}$. For 3 of 9 (33%) compounds, the error was in the range of 3- to 10-fold.

Discussion

The prediction of human PK parameters is an important step during the preclinical development of pharmaceuticals to reduce costs by enabling the early elimination of candidates with unsuitable properties. However, species differences make it difficult to predict human PK from animal data; monkey data may lead to underprediction (Chiou and Buehler, 2002; Akabane et al., 2010), whereas dog data may cause overestimation (Chiou et al., 2000). In vitro-in vivo scaling from data obtained with human hepatic microsomes and hepatocytes is a widely used approach but often results in the underprediction of in vivo CL (Obach, 1999). We considered the possibility that PXB mice, in which hepatocytes are replaced with human hepatocytes to the extent of approximately 80% (Tateno et al., 2004), may have superior predictive utility, because the expression levels and activities of both P450 and non-P450 enzymes well reflect those of the donor hepatocytes (Yoshitsugu et al., 2006; Yamasaki et al., 2010). In this study, we checked metabolic activities (CYP2C9, CYP2D6, UGT, SULT, and AO) using probe substrates between donor hepatocytes and h-hepatocytes purified from PXB mice (Supplemental Table 3) as well as the expression of drug transporters and blood albumin (Tateno et al., 2004; Nishimura et al., 2005).

For the present study, we selected 13 model compounds with diverse chemical structures (Fig. 1), which are metabolized through multiple pathways by P450 and non-P450 enzymes, such as UGT, SULT, and AO. Their values of CL cover a wide range from 0.055 to 118 ml · min^{-1} · kg^{-1} (Table 1).

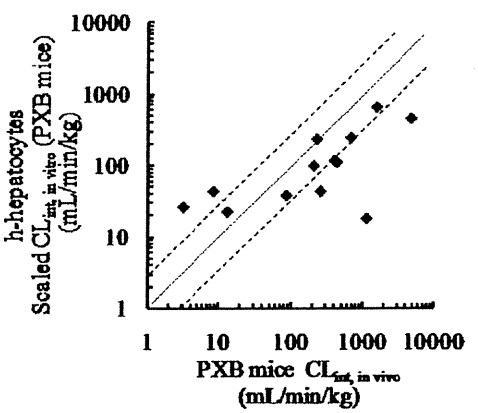

FIG. 4. Correlation between $CL_{int,in\ vivo}$ of PXB mice and $CL_{int,in\ vitro}$ of their hepatocytes, calculated as described in the text. The solid line represents unity. The dotted line represents the range within 3-fold of unity.

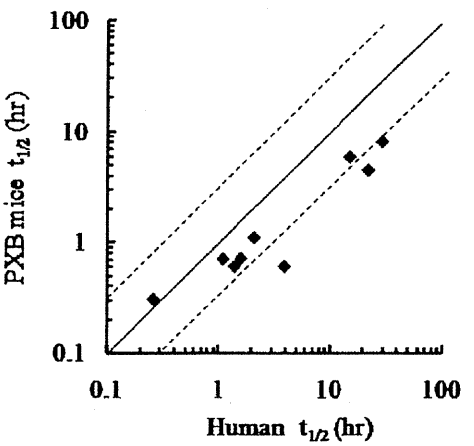

FIG. 6. Correlation of $t_{1/2}$ after intravenous administration between humans and PXB mice. Compounds for which literature data were not available were excluded from this figure. The solid line represents unity. The dotted line represents the range within 3-fold of unity.

First, we performed an in vitro metabolic study using fresh h-hepatocytes isolated from PXB mice. We calculated $CL_{int,in\ vitro}$ using fresh h-hepatocytes and compared the results with human $CL_{int,in\ vivo}$ estimated by use of a well stirred model (Pang and Rowland, 1977). These results using a parallel tube model and a dispersion model were also similar to those of a well stirred model (S. Sanoh, unpublished observations). A moderate correlation ($r^2 = 0.475$, $p = 0.009$) was found, but this approach was not superior to prediction using other methods.

$CL_{int,in\ vitro}$ values of diclofenac, ibuprofen, warfarin, and zaleplon were approximately similar to reported values using cryopreserved hepatocytes (Ekins and Obach, 2000; Nagilla et al., 2006; Stringer et al., 2008), supporting the idea that $CL_{int,in\ vitro}$ values are similar in fresh hepatocytes and cryopreserved hepatocytes (Naritomi et al., 2003; McGinnity et al., 2004).

A similar correlation ($r^2 = 0.435$, $p = 0.014$) was observed between $CL_{int,in\ vitro}$ and $CL_{int,in\ vivo}$ in PXB mice (Fig. 4). In both cases, the numbers of compounds for which absolute values of CL_{int} were predicted within a 3-fold error were insufficient.

Therefore, we next evaluated the predictability of hepatic clearance and $t_{1/2}$ from in vivo data in PXB mice. The values of $CL_{int,in\ vivo}$ estimated by intravenous administration in PXB mice were well correlated ($r^2 = 0.754$, $p = 1.174 \times 10^{-4}$) with observed $CL_{int,in\ vivo}$ in human. Surprisingly, we also found a good correlation ($r^2 = 0.886$, $p = 1.506 \times 10^{-4}$) between $t_{1/2}$ values in PXB mice and humans. However, although the rank order was the same, there were rather large prediction errors, so it may not be possible to predict absolute values. This is consistent with the findings of Xiao et al. (2010) in PXB mice.

We used PXB mice that showed that the average RI values were approximately 80%. It was a concern that the contribution of the remaining approximately 20% mice hepatocytes may be reflected on clearance. $CL_{int,in\ vitro}$ values of these model compounds in host mice hepatocytes (severe combined immunodeficiency mice) were almost higher than those of h-hepatocytes within a 10-fold range (Supplemental Fig. 1). The extent of the difference may not influence the predictability of $CL_{int,in\ vivo}$.

For the estimation of $CL_{int,in\ vivo}$ in PXB mice, the fu values of those model compounds is the same as those in humans because human albumin is expressed in the blood of PXB mice. Inoue et al. (2009) reported fu value of warfarin in PXB mice was similar to that in humans. Furthermore, fu values of some compounds (dapsone, diclofenac, ketoprofen, salbutamol, and zaleplon) in this study were also approximately similar to those in humans (S. Sanoh, unpublished observations).

We assumed that the Rb values of those model compounds is also the same as those in humans, because Rb values of some compounds (dapsone, diclofenac, ketoprofen, salbutamol, and zaleplon) in this study were also approximately similar to those in humans (S. Sanoh, unpublished observations).

Q values were assumed to be 90 ml $\cdot$ min^{-1} $\cdot$ kg^{-1}, respectively, corresponding to the values of normal mice (Davies and Morris, 1993). In further work, it would be desirable to examine whether these values are appropriate.

In this study, we selected model compounds metabolized not only by P450, but also by non-P450 enzymes, including AO. 6-Deoxypenciclovir, fasudil, sulindac, and zaleplon are metabolized mainly by AO in humans. It has been reported that human CL for drugs metabolized by AO may be underpredicted from data obtained with human liver cytosol and S9 due to the loss or deactivation of AO during preparation, homogenization, storage, and experimental procedures (Zientek et al., 2010). PXB mice have high AO activity, being similar to humans (Kitamura et al., 2008), and may be a useful source of fresh h-hepatocytes.

Our results indicate that PXB mice can be used at least for semiquantitative prediction of not only CL_i but also $t_{1/2}$ in humans. PXB mice also would be useful for in vitro estimation and comparison of PK of various candidate compounds, because large amounts of fresh, identical hepatocytes (1.1×10^8 cells/mouse) are available by transplantation of donor hepatocytes (2.5×10^5 cells/mouse). The combination of in vitro study in PXB mice and in vitro study using PXB hepatocytes may prove to be particularly effective.

Acknowledgments

We thank members in PhoenixBio Co., Ltd. for the isolation of hepatocytes from PXB mice.

Authorship Contributions

Participated in research design: Sanoh, Sugihara, Kotake, Tayama, Horie, Kitamura, and Ohta.

Conducted experiments: Sanoh and Horiguchi.

Contributed new reagents or analytic tools: Sugihara, Ohshita, and Tateno.

Performed data analysis: Sanoh and Horiguchi.

Wrote or contributed to the writing of the manuscript: Sanoh, Kotake, Tateno, and Ohta.

References

Akabane T, Tabata K, Kadono K, Sakuda S, Terashita S, and Teramura T (2010) A comparison of pharmacokinetics between humans and monkeys. *Drug Metab Dispos* **38**:308–316.

Brown HS, Griffin M, and Houston JB (2007) Evaluation of cryopreserved human hepatocytes as an alternative in vitro system to microsomes for the prediction of metabolic clearance. *Drug Metab Dispos* **35**:293–301.

Chiba M, Ishii Y, and Sugiyama Y (2009) Prediction of hepatic clearance in human from in vitro data for successful drug development. *AAPS J* **11**:262–276.

Chiou WL and Buehler PW (2002) Comparison of oral absorption and bioavailability of drugs between monkey and human. *Pharm Res* **19**:868–874.

Chiou WL, Jeong HY, Chung SM, and Wu TC (2000) Evaluation of using dog as an animal model to study the fraction of oral dose absorbed of 43 drugs in humans. *Pharm Res* **17**:135–140.

Davies B and Morris T (1993) Physiological parameters in laboratory animals and humans. *Pharm Res* **10**:1093–1095.

De Buck SS, Sinha VK, Fenu LA, Nijsen MJ, Mackie CE, and Gilissen RA (2007) Prediction of human pharmacokinetics using physiologically based modeling: a retrospective analysis of 26 clinically tested drugs. *Drug Metab Dispos* **35**:1766–1780.

De Series M, Bowers G, Boyle G, Beaumont C, Castellino S, Sigalotos J, Dave M, Roberts A, Shah V, Olson K, et al. (2011) Evaluation of a chimeric (uPA+/+/SCID mouse model with a humanized liver for prediction of human metabolism. *Xenobiotica* **41**:464–475.

Ekins S and Obach RS (2000) Three dimensional quantitative structure activity relationship computational approaches for prediction of human in vitro intrinsic clearance. *J Pharmacol Exp Ther* **295**:463–473.

Fagerholm U (2007) Prediction of human pharmacokinetics: evaluation of methods for prediction of hepatic metabolic clearance. *J Pharm Pharmacol* **59**:803–828.

Hallifax D, Foster JA, and Houston JB (2010) Prediction of human metabolic clearance from in vitro systems: retrospective analysis and prospective view. *Pharm Res* **27**:2150–2161.

Huang L, Berry L, Ganga S, Janosky B, Chen A, Roberts J, Colletti AE, and Lin MH (2010) Relationship between passive permeability, efflux, and predictability of clearance from in vitro metabolic intrinsic clearance. *Drug Metab Dispos* **38**:223–231.

Inoue T, Sugihara K, Ohshita H, Horie T, Kitamura S, and Ohta S (2009) Prediction of human disposition toward S-3H-warfarin using chimeric mice with humanized liver. *Drug Metab Pharmacokinet* **24**:153–160.

Kamimura H, Nakada N, Suzuki K, Mera A, Souda K, Murakami Y, Tanaka K, Iwatsubo T, Kawamura A, and Usui T (2010) Assessment of chimeric mice with humanized liver as a tool for predicting circulating human metabolites. *Drug Metab Pharmacokinet* **25**:223–235.

Katoh M, Matsui T, Nakajima M, Tateno C, Kataoka M, Soeno Y, Horie T, Iwaoka K, Yoshizato K, and Yokoi T (2004) Expression of human cytochromes P450 in chimeric mice with humanized liver. *Drug Metab Dispos* **32**:1402–1410.

Katoh M, Matsui T, Okumura H, Nakajima M, Nishimura M, Naito S, Tateno C, Yoshizato K, and Yokoi T (2005) Expression of human phase II enzymes in chimeric mice with humanized liver. *Drug Metab Dispos* **33**:1333–1340.

Kitamura S, Nitta K, Tayama Y, Tanoue C, Sugihara K, Inoue T, Horie T, and Ohta S (2008) Aldehyde oxidase-catalyzed metabolism of N1-methylnicotinamide in vivo and in vitro in chimeric mice with humanized liver. *Drug Metab Dispos* **36**:1202–1205.

McGinnity DF, Soars MG, Urbanowicz RA, and Riley RJ (2004) Evaluation of fresh and cryopreserved hepatocytes as in vitro drug metabolism tools for the prediction of metabolic clearance. *Drug Metab Dispos* **32**:1247–1253.

Nagilla R, Frank KA, Johvette LJ, and Ward KW (2006) Investigation of the utility of published in vitro intrinsic clearance data for prediction of in vivo clearance. *J Pharmacol Toxicol Methods* **53**:106–116.

Naritomi Y, Terashita S, Kagayama A, and Sugiyama Y (2003) Utility of hepatocytes in predicting drug metabolism: comparison of hepatic intrinsic clearance in rats and humans in vivo and in vitro. *Drug Metab Dispos* **31**:580–588.

Nishimura M, Yoshitsugu H, Yokoi T, Tateno C, Kataoka M, Horie T, Yoshizato K, and Naito

S (2005) Evaluation of mRNA expression of human drug-metabolizing enzymes and transporters in chimeric mouse with humanized liver. *Xenobiotica* **35**:877–890.

Obach RS (1999) Prediction of human clearance of twenty-nine drugs from hepatic microsomal intrinsic clearance data: An examination of in vitro half-life approach and nonspecific binding to microsomes. *Drug Metab Dispos* **27**:1350–1359.

Paixão P, Gouveia LF, and Morais JA (2010) Prediction of the in vitro intrinsic clearance determined in suspensions of human hepatocytes by using artificial neural networks. *Eur J Pharm Sci* **39**:310–321.

Pang KS and Rowland M (1977) Hepatic clearance of drugs. I. Theoretical considerations of a "well-stirred" model and a "parallel tube" model. Influence of hepatic blood flow, plasma and blood cell binding, and the hepatocellular enzymatic activity on hepatic drug clearance. *J Pharmacokinet Biopharm* **5**:625–653.

Stringer R, Nicklin PL, and Houston JB (2008) Reliability of human cryopreserved hepatocytes and liver microsomes as in vitro systems to predict metabolic clearance. *Xenobiotica* **38**:1313–1329.

Tabata K, Hamakawa N, Sanoh S, Terasuna S, and Teramura T (2009) Exploratory population pharmacokinetics (e-PPK) analysis for predicting human PK using exploratory ADME data during early drug discovery research. *Eur J Drug Metab Pharmacokinet* **34**:117–128.

Tateno C, Yoshizane Y, Saito N, Kataoka M, Utoh R, Yamasaki C, Tachibana A, Soeno Y, Asahina K, Hino H, et al. (2004) Near completely humanized liver in mice shows human-type metabolic responses to drugs. *Am J Pathol* **165**:901–912.

Wang Q, Jia R, Ye C, Garcia M, Li J, and Hidalgo IJ (2005) Glucuronidation and sulfation of 7-hydroxycoumarin in liver matrices from human, dog, monkey, rat, and mouse. *In Vitro Cell Dev Biol Anim* **41**:97–103.

Xiao G, Bohnert T, Black C, Klunk L, and Gan LS (2010) Evaluation of chimeric mice with humanized liver to predict human intrinsic clearance of drug molecules at preclinical phase. *Drug Metab Rev* **42(S1:)**P60.

Yamasaki C, Kataoka M, Kato Y, Kakuni M, Usuda S, Ohzone Y, Matsuda S, Adachi Y, Ninomiya S, Itamoto T, et al. (2010) In vitro evaluation of cytochrome P450 and glucuronidation activities in hepatocytes isolated from liver-humanized mice. *Drug Metab Pharmacokinet* **25**:539–550.

Yamazaki H, Kuribayashi S, Inoue T, Tateno C, Nishikura Y, Oofusa K, Harada D, Naito S, Horie T, and Ohta S (2010) Approach for in vivo protein binding of 5-n-butyl-pyrazolo[1,5-a]pyrimidine bioactivated in chimeric mice with humanized liver by two-dimensional electrophoresis with accelerator mass spectrometry. *Chem Res Toxicol* **23**:152–158.

Yoshitsugu H, Nishimura M, Tateno C, Kataoka M, Takahashi E, Soeno Y, Yoshizato K, Yokoi T, and Naito S (2006) Evaluation of human CYP1A2 and CYP3A4 mRNA expression in hepatocytes from chimeric mice with humanized liver. *Drug Metab Pharmacokinet* **21**:465–474.

Zientek M, Jiang Y, Youdim K, and Obach RS (2010) In vitro-in vivo correlation for intrinsic clearance for drugs metabolized by human aldehyde oxidase. *Drug Metab Dispos* **38**:1322–1327

Address correspondence to: Dr. Seigo Sanoh, Graduate School of Biomedical Sciences, Hiroshima University, Kasumi 1-2-3, Minami-ku, Hiroshima 734-8553 Japan. E-mail: sanoh@hiroshima-u.ac.jp

DMD DRUG METABOLISM AND DISPOSITION aspet

1521-009X/12/4003-474-480$25.00
DRUG METABOLISM AND DISPOSITION
Copyright © 2012 by The American Society for Pharmacology and Experimental Therapeutics
DMD 40:474–480, 2012

Vol. 40, No. 3
42754/3748075

DMD
DRUG METABOLISM AND DISPOSITION
aspet

Investigation of Drug-Drug Interactions Caused by Human Pregnane X Receptor-Mediated Induction of CYP3A4 and CYP2C Subfamilies in Chimeric Mice with a Humanized Liver[S]

Maki Hasegawa, Harunobu Tahara, Ryo Inoue, Masakazu Kakuni, Chise Tateno, and Junko Ushiki

Kyowa Hakko Kirin Co., Ltd., Nagaizumi-cho, Sunto-gun, Shizuoka, Japan (M.H., H.T., J.U.); and PhoenixBio, Co., Ltd., Higashihiroshima-shi, Hiroshima, Japan (R.I., M.K., C.T.)

Received September 14, 2011; accepted November 29, 2011

ABSTRACT:

The induction of cytochrome P450 (P450) enzymes is one of the risk factors for drug-drug interactions (DDIs). To date, the human pregnane X receptor (PXR)-mediated CYP3A4 induction has been well studied. In addition to CYP3A4, the expression of CYP2C subfamily is also regulated by PXR, and the DDIs caused by the induction of CYP2C enzymes have been reported to have a major clinical impact. The purpose of the present study was to investigate whether chimeric mice with a humanized liver (PXB mice) can be a suitable animal model for investigating the PXR-mediated induction of CYP2C subfamily, together with CYP3A4. We evaluated the inductive effect of rifampicin (RIF), a typical human PXR ligand, on the plasma exposure to the four P450 substrate drugs (triazolam/CYP3A4, pioglitazone/CYP2C8, (*S*)-warfarin/CYP2C9, and (*S*)-(−)-mephenytoin/CYP2C19) by cassette dosing in PXB mice. The induction of several drug-metabolizing enzymes and transporters in the liver was also examined by measuring the enzyme activity and mRNA expression levels. Significant reductions in the exposure to triazolam, pioglitazone, and (*S*)-(−)-mephenytoin, but not to (*S*)-warfarin, were observed. In contrast to the in vivo results, all the four P450 isoforms, including CYP2C9, were elevated by RIF treatment. The discrepancy in the (*S*)-warfarin results between in vivo and in vitro studies may be attributed to the relatively small contribution of CYP2C9 to (*S*)-warfarin elimination in the PXB mice used in this study. In summary, PXB mice are a useful animal model to examine DDIs caused by PXR-mediated induction of CYP2C and CYP3A4.

Introduction

The induction of cytochrome P450 (P450) enzymes is one of the risk factors for drug-drug interactions (DDIs) (Niemi et al., 2003; Luo et al., 2004). The human pregnane X receptor (PXR) is a key nuclear receptor principally responsible for the induction of several P450 enzymes, including CYP3A4, -2C8, -2C9, -2C19, -2A6, and -2B6 (Niemi et al., 2003; Sinz et al., 2008; Chen and Goldstein, 2009). In addition to P450 enzymes, the expression of several drug transporters, such as multidrug resistance gene (MDR) 1, multidrug resistance-associated protein (MRP) 2, organic anion-transporting polypeptides, and phase II metabolic enzymes, including UDP-glucuronosyltransferase (UGT), sulfotransferase, and glutathione S-transferase, are also regulated by human PXR (Dixit et al., 2007; Nishimura et al., 2008a,b; Sinz et al., 2008).

In humans, CYP3A4 plays a major role in drug metabolism because of its abundant expression in the liver and intestine and its broad substrate specificity. In fact, CYP3A4 contributes to the oxidative metabolism of more than 50% of all currently used drugs (de Wildt et al., 1999; Luo et al., 2004). Therefore, CYP3A4-related DDIs have a major clinical impact. CYP3A4 is the most studied isoform among the P450s in terms of DDIs caused by PXR-related induction of drug-metabolizing enzymes. Both in vitro and in vivo experimental models for CYP3A4 induction have been reported by several pharmaceutical companies (Cui et al., 2008; Kanebratt and Andersson, 2008; Kim et al., 2008, 2010; Kamiguchi et al., 2010).

The human CYP2C subfamily has four members: CYP2C8, CYP2C9, CYP2C18, and CYP2C19 (Lüpple et al., 2003; Chen and Goldstein, 2009). Of these, CYP2C8, CYP2C9, and CYP2C19 are of clinical importance and are collectively responsible for the metabolism of ~20% of clinically used drugs (Chen and Goldstein, 2009). The substrate specificity of CYP3A4 and CYP2C enzymes sometimes overlaps. In that case, the overall contribution of PXR-regulated P450 enzymes in the drug elimination process is relatively large. These observations suggest that new investigations should focus on the DDIs

Article, publication date, and citation information can be found at http://dmd.aspetjournals.org.
http://dx.doi.org/10.1124/dmd.111.042754.
[S] The online version of this article (available at http://dmd.aspetjournals.org) contains supplemental material.

ABBREVIATIONS: P450, cytochrome P450; DDI, drug-drug interaction; PXR, pregnane X receptor; MDR, multidrug resistance gene; MRP, multidrug resistance-associated protein; UGT, UDP-glucuronosyltransferase; RIF, rifampicin; ROS, rosiglitazone; WAR, (*S*)-warfarin; MEP, (*S*)-(−)-mephenytoin; TRZ, triazolam; GAPDH, glyceraldehyde-3-phosphate dehydrogenase; PCR, polymerase chain reaction; G-6-P, D-glucose 6-phosphate; G-6-P-DH, G-6-P dehydrogenase; LC/MS/MS, liquid chromatography-tandem mass spectrometry; AUC, area under the plasma concentration-time curve.

between PXR ligands and CYP2C substrate drugs. The quantitative polymerase chain reaction (PCR) analyses using human hepatocytes have demonstrated that the magnitude of CYP3A4 induction by PXR ligand is the largest followed by CYP2C enzymes, including CYP2C8, CYP2C9, and CYP2C19 (Raucy et al., 2002; Niemi et al., 2003). In fact, DDIs caused by induction of CYP2C enzymes have been also reported (Chen and Goldstein, 2009). However, there has been no systematic in vivo analysis focusing on the differences in the degree of the inductive effects of PXR ligands on the each of these P450 enzymes.

It has been reported that there is a large species difference in ligand recognition by the PXR between rodents and humans (Jones et al., 2000; LeCluyse, 2001). For example, RIF is more selective for human PXR, whereas the synthetic C21 steroid pregnenolone-16[propio]-carbonitrile, is a weak ligand for the human PXR but a potent ligand for rodents (Jones et al., 2000; LeCluyse, 2001). In fact, the expression of mouse Cyp3a is not influenced by the administration of RIF (Ma et al., 2007). The species differences in the ligand recognition of the PXR limit the utility of animal models to predict PXR-related DDIs in humans. In addition, it is known that there are species differences in metabolic patterns, as well as in the contribution of each P450 isoform to drug elimination (Shin et al., 2009; Kanimura et al., 2010). These species differences make it hard to predict human pharmacokinetics from animal data. Recently, several groups, including our own, have generated the humanized mouse models of the PXR and CYP3A4 by gene knockout and transgenic techniques (Xie et al., 2000; Ma et al., 2007; Kim et al., 2008; Scheer et al., 2008; Hasegawa et al., 2011). These models are useful for investigating CYP3A4 induction by human PXR ligands. However, the effect of the human PXR ligand on drug-metabolizing enzymes other than CYP3A4 cannot be examined using these mouse models.

The chimeric mouse with a humanized liver is an alternative mouse model (Strom et al., 2010). This mouse model, designated as the "PXB mouse," has been established by the transplantation of human hepatocytes into urokinase-type plasminogen activator-transgenic severe combined immunodeficient mice (Tateno et al., 2004). The livers of the PXB mice are replaced with more than 70% human hepatocytes, although the remaining 30% are mouse hepatocytes (Strom et al., 2010). It has been reported that the mRNA expression of several P450 enzymes in the PXB mouse liver is induced by RIF treatment and that PXB mice also show similar drug-metabolizing profiles of CYP3A4 and CYP2C substrate drugs to humans (Katoh et al., 2005a,b; Kanimura et al., 2010). The PXB mouse is expected to provide the opportunity to examine the inductive effect of PXR ligands on the plasma profiles of not only CYP3A4 but also CYP2C substrate drugs. This study will provide important information on DDIs caused by CYP2C induction in addition to CYP3A4.

In the present study, we evaluated the inductive effect of three different doses of RIF on the plasma exposure of PXB mice to the substrate drugs of CYP3A4, CYP2C8, CYP2C9, and CYP2C19, which have been reported to have DDIs with RIF in humans. Furthermore, the induction of several drug-metabolizing enzymes and transporters in the liver was also examined by measuring the enzyme activities and mRNA expression levels.

Materials and Methods

Materials. RIF, rosiglitazone (ROS), (*S*)-warfarin (WAR), dextromethorphan hydrobromide monohydrate, and propranolol hydrochloride were purchased from Wako Pure Chemical Industries (Osaka, Japan). Triazolam (TRZ), phenacetin, bupropion, and diclofenac were purchased from Sigma-Aldrich (St. Louis, MO). (*S*)-(−)-Mephenytoin (MEP) was purchased from Toronto Research Chemicals (North York, Canada). $NADP^+$, D-glucose 6-phosphate (G-6-P), and G-6-P dehydrogenase (G-6-P-DH) were purchased from Oriental Yeast (Tokyo, Japan). All other chemicals and solvents were of analytical grade otherwise noted.

Generation of Chimeric Mice with a Humanized Liver. All animal studies were conducted in accordance with the *Guiding Principles for the Care and Use of Laboratory Animals*, and the experimental protocol used in this study was approved by the Committee for Animal Experiments of PhoenixBio Co., Ltd., and Kyowa Hakko Kirin Co., Ltd. The PXB mice were generated as described previously (Tateno et al., 2004). All PXB mice used in the present study were derived from the same donor cryopreserved hepatocytes (BD85, from a 5-year-old black male; BD Biosciences, Franklin Lakes, NJ). The blood concentration of human albumin in the PXB mice was measured according to a previous report (Tateno et al., 2004) to predict the replacement index of human hepatocytes that had repopulated in the host mouse liver. The actual values of the replacement index in PXB mice used in this study ranged from 82 to 94%.

Pharmacokinetic DDI Study in PXB Mice. Male PXB mice (11–12-weeks-old, 18–23 g) were used in this study. The suspensions of RIF prepared with corn oil were given intraperitoneally at doses of 2, 10, and 50 mg/kg to the PXB mice once daily for 4 days. After the 4 days of treatment of RIF, the PXB mice received a mixture of CYP3A4, CYP2C8, CYP2C9, and CYP2C19 substrate drugs orally via cassette dosing. The dosing mixture was prepared by adding a dimethyl sulfoxide solution of each drug to a 0.5% methylcellulose aqueous solution. The dose of each substrate drug was as follows: TRZ (CYP3A4 substrate), 5 mg/kg; ROS (CYP2C8 substrate), 1 mg/kg; WAR (CYP2C9 substrate), 0.1 mg/kg; and MEP (CYP2C19 substrate), 5 mg/kg. Blood samples were collected at 2 h after administration on days 1 and 4 and 0.5, 1, 2, 4, and 7 h on day 5. The blood samples were centrifuged, and the plasma samples obtained were stored at −80°C until the analysis. After blood sampling on day 5, the mice were euthanized, and a piece of the liver was collected and preserved in RNAlater solution (Invitrogen, Carlsbad, CA) to stabilize the RNA. The remaining liver tissue was frozen in liquid nitrogen and stored at −80°C until microsomal preparation.

RNA Isolation and Quantitative Reverse Transcription-PCR. Total RNA was extracted from the liver using an RNeasy Plus mini kit (QIAGEN, Hilden, Germany) and was reverse-transcribed to obtain cDNA using a PrimeScript RT reagent kit (Takara Bio, Shiga, Japan) according to the manufacturer's instructions. SYBR-PCR was performed using an ABI PRISM 7900HT (Invitrogen) with SYBR Premix Ex Taq (Takara Bio). The PCR conditions were as follows: after initial denaturation at 94°C for 5 min, the amplification was performed by denaturation at 94°C for 30 s, annealing at 65°C for 30 s, and extension at 72°C for 30 s for 45 cycles. In all cases, the input cDNA concentrations were normalized to those of glyceraldehyde-3-phosphate dehydrogenase (GAPDH; ΔCt). The relative mRNA expression was determined by a $2^{-\Delta\Delta Ct}$ calculation. The primer sequences used in the present study are summarized in Table 1. We confirmed that these primers were capable of amplifying human but not mouse genes.

Preparation of Liver Microsomes and Metabolic Assay. Liver microsomes were prepared from the frozen liver tissues as described previously (Sugihara et al., 2001). The reaction conditions for the enzyme activity of each P450 isoform are summarized in Table 2. The optimized substrate concentrations, the microsomal concentrations, and the reaction times were used to determine metabolic activity precisely. A reaction mixture (50 μl) consisted of 100 mM phosphate buffer, pH 7.4, 3 mM magnesium chloride, 8 mM G-6-P, 1 U/ml G-6-P-DH, 0.8 mM $NADP^+$, microsomal protein, and substrate. The reaction was initiated by the addition of an NADPH-generating system (a mixture of magnesium chloride, G-6-P, G-6-P-DH, and $NADP^+$) after preincubation of the mixture without the NADPH-generating system for 5 min at 37°C. The reaction was terminated at the designated time by the addition of ice-cold methanol containing propranolol as an internal standard. The sample was centrifuged, and the supernatant was diluted with water. The metabolite of each substrate was analyzed using a liquid chromatography-tandem mass spectrometry (LC/MS/MS) system.

Pretreatment of Plasma. Two microliters of plasma sample, 2 μl of dimethyl sulfoxide, and 30 μl of the ice-cold methanol containing the internal standard were mixed and centrifuged. The calibration standards were prepared in the same manner as the plasma samples. The supernatant was mixed with 10

TABLE 1

The sequences of the primers for SYBR-PCR

Gene Name	Primer Sequence (5′ 3′)	
	Forward	Reverse
CYP1A2	AGCTTGACCTTCAGCACAGAC	GATAGTGCTCCTGGACTGTTTTC
CYP2B6	CACTCATCAGCTCTGTATTCGG	GTATGGCATTTTGGCTCGG
CYP2C8	CACAGCTAAAGTCCAGGAAGAC	GATGGGCTAGCATTCTTCAGAC
CYP2C9	ACTATCTCATTCCCAAGGCAC	GTTCACTAGATCTTCAGGGAAGGC
CYP2C19	CAGCTGACTTACTTGGAGCTGG	CCTGCTGAGAAAGGCATGAAG
CYP2D6[a]	GGTGTGACCCATATGACATC	CTCCCCGAGGCATGCACG
CYP3A4	AGTTAATCCACTGTGACTTTGCCC	TCAGGATGGAATGCAAGAGG
UGT1A1	TGTTCCCACTTACTGCACAAC	CTTCAAATTCCTGGGATAGTGG
MDR1	GTATTCAACTATCCCACCCGAC	GAGCTGAGTTCCTTTGTCTCCTAC
MRP2	ACATGAGAGTTGGAGTCTACGG	GGATAACTGGCAAACCTGATAC
GAPDH	CCGAGCCACATCGCTCAGAC	ATGACGAACATGGGGGCATCAG

[a] From Kaboh et al. (2005a).

mM ammonium acetate, and the mixture was injected into the LC/MS/MS system.

LC/MS/MS Analysis. The concentrations of the substrate drugs (in plasma samples), and metabolites (in microsomal samples) were measured using the LC/MS/MS system consisting of an ACQUITY UPLC (Waters, Inc., Bedford, MA) connected to a 4000 QTRAP mass spectrometer (AB Sciex, Foster City, CA).

For the plasma samples, chromatographic separation was performed on a CAPCELL PAK C18 MGII column (3 μm, 3 mm inner diameter × 35 mm; Shiseido, Tokyo, Japan) using an injection volume of 10 μl (ROS and WAR) or 25 μl (TRZ and MEP) and a run time of 4 min. The elution was conducted at a flow rate of 0.8 ml/min by a linear gradient with the mobile phase, which consisted of 10 mM ammonium acetate in water (A) and methanol (B). The gradient condition of B (%) was as follows: at 0, 0.2, 2.2, 2.21, 3, and 3.01 min, the B% was 80, 80, 25, 10, 10, and 80%, respectively. The mass spectrometry detection was performed by positive ionization electrospray. The multiple reaction monitoring mode was used, and the monitor ions (*m/z* precursor ion > product ion) were as follows: ROS (358.1 > 153.3), WAR (309.6 > 163.5), TRZ (343.4 > 308.1), and MEP (219.6 > 134.4). The plasma concentration ranges of quantification were as follows: ROS (1.07–3570 ng/ml), WAR (0.925–9250 ng/ml), TRZ (0.343–3430 ng/ml), and MEP (2.18–6550 ng/ml).

For the microsomal samples, chromatographic separation was performed on an ACQUITY UPLC BEH C18 column (1.7 μm, 2.1 mm inner diameter × 50 mm; Waters, Milford, MA) using an injection volume of 7.5 μl and a run time of 2.5 min. The elution was conducted at a flow rate of 0.5 ml/min by a linear gradient with the mobile phase, which consisted of 10 mM ammonium acetate in water (A for CYP1A2, CYP2B6, CYP2C9 (7-hydroxywarfarin), CYP2C19, and CYP2D6 assays) or 0.05% formic acid in water (A for CYP2C8, CYP2C9 (4′-hydroxydiclofenac), and CYP3A4 assays) and methanol (B). The gradient condition of B (%) was as follows: at 0, 0.2, 1.5, 2 and 2.01 min, the B% was 95, 95, 5, 5, and 95%, respectively. The mass spectrometry detection was performed by positive ionization electrospray. The multiple reaction monitoring mode was used, and the monitor ions (*m/z* precursor ion > product ion) were as follows: CYP1A2 (acetaminophen, 152.0 > 110.0), CYP2B6 (hydroxybupropion, 256.1 > 238.1), CYP2C8 (*N*-demethyl rosiglitazone, 344.1 > 121.1; 5-hydroxyrosiglitazone, 374.1 > 151.1), CYP2C9 (4′-hydroxydiclofenac, 312.05 > 230.45; 7-hydroxywarfarin, 325.6 > 163.5), CYP2C19 (4′-hydroxymephenytoin, 235.0 > 150.15), CYP2D6 (dextrorphan, 258.1 > 157.1), and CYP3A4 (1′-hydroxytriazolam, 359.1 > 176.1; 4-hydroxytriazolam, 359.1 > 314.1). Although the metabolites concentrations in the microsomal samples were not quantified, we have confirmed the linearity of signal intensities and no signals in the blank samples.

Pharmacokinetic Analysis. The pharmacokinetic parameters for TRZ, ROS, WAR, and MEP were obtained by a noncompartmental analysis. The log-transformed plasma concentrations were plotted against time. The slope of the elimination phase (λ_z) was estimated by linear regression. The maximal plasma concentration (C_{max}) and time to C_{max} (t_{max}) were obtained directly from the observed values. The apparent $t_{1/2}$ was obtained as $\ln 2/\lambda_z$. The area under the plasma concentration-time curve (AUC) from time 0 to the last data point (AUC_{0-t}) was calculated using the linear trapezoidal method. The AUC after the last data point ($AUC_{\lambda z}$) was estimated by extrapolating with λ_z. The sum of AUC_{0-t} and $AUC_{\lambda z}$ was regarded as $AUC_{0-\infty}$.

Statistical Analysis. A one-way analysis of variance with a Dunnett's test was performed to assess for significant differences in the pharmacokinetics, metabolic activity in the liver microsomes, and mRNA expression in the liver between vehicle- and RIF-treated groups. The statistical analyses were performed using the SAS software program (SAS Institute, Cary, NC). The criterion for statistical significance was $P < 0.05$.

Results

The Effect of RIF Treatment on the Pharmacokinetics of CYP3A4 and CYP2C Substrate Drugs. The pharmacokinetics of CYP3A4 (TRZ) and CYP2C substrate drugs (ROS, MEP, and WAR) was evaluated after repeated intraperitoneal administration of RIF (2, 10, and 50 mg/kg daily for 4 days) or vehicle to the PXB mice. The plasma concentration-time profiles of the substrate drugs are shown in Fig. 1, and the pharmacokinetic parameters and the AUC decrease (percentage) of substrate drugs are summarized in Table 3. The plasma exposure to TRZ was decreased with increased doses of RIF

TABLE 2

The reaction conditions for P450 enzyme assay using the liver microsomes

P450	Substrate	Metabolite	Substrate Concentration	Microsomal Concentration	Reaction Time
			μM	*mg/ml*	*min*
CYP1A2	Phenacetin	Acetaminophen	5	0.5	20
CYP2B6	Bupropion	Hydroxybupropion	5	0.5	20
CYP2C8	Rosiglitazone	*N*-Demethylrosiglitazone 5-Hydroxyrosiglitazone	2	0.2	20
CYP2C9	(*S*)-Warfarin	7-Hydroxywarfarin	4	1	30
	Diclofenac	4′-Hydroxydiclofenac	4	0.2	30
CYP2C19	(*S*)-(−)-Mephenytoin	4′-Hydroxymephenytoin	20	0.5	20
CYP2D6	Dextromethorphan	Dextrorphan	1	0.2	20
CYP3A4	Triazolam	1′-Hydroxytriazolam 4-Hydroxytriazolam	2	0.2	20

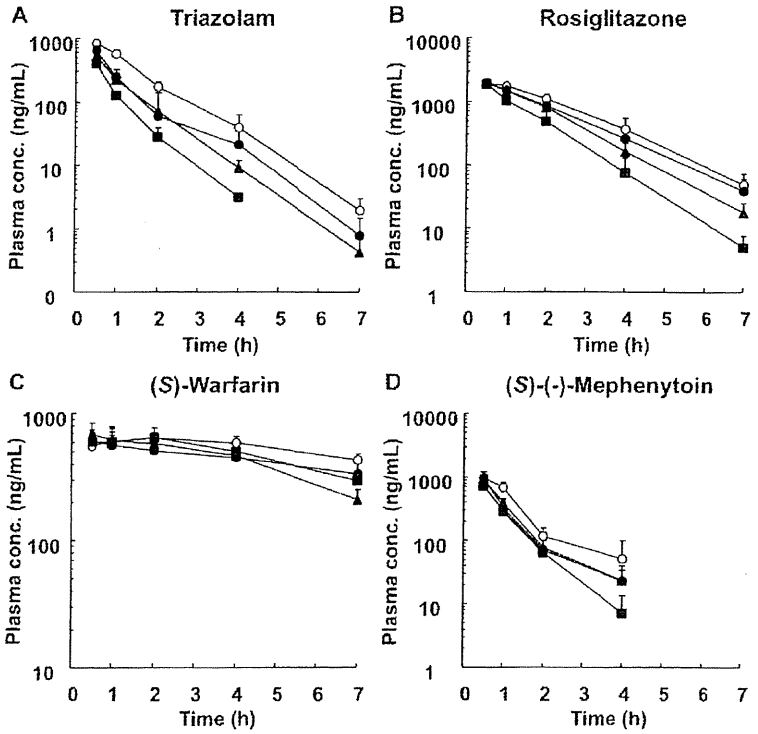

Fig. 1. The plasma concentration-time profiles of TRZ (A), ROS (B), WAR (C), and MEP (D) after repeated intraperitoneal administration of RIF once daily for 4 days to male PXB mice. The PXB mice were given oral doses of 5 mg/kg TRZ (CYP3A4 substrate), 1 mg/kg ROS (CYP2C8 substrate), 0.1 mg/kg WAR (CYP2C9 substrate), and 5 mg/kg MEP (CYP2C19 substrate) via cassette dosing after 4 days of treatment with 2 (●), 10 (▲), or 50 (■) mg/kg RIF or vehicle (○). Each point represents the mean ± S.D. of three mice.

(Fig. 1A). The TRZ AUC was significantly decreased by 46 (2 mg/kg), 54 (10 mg/kg), and 71% (50 mg/kg) compared with the vehicle control (Table 3). RIF treatment also resulted in an AUC decrease of ROS and MEP with increased doses of RIF, and the statistically significance in the AUC decrease was observed only at the dose of 50 mg/kg RIF as 47% for ROS and 46% for MEP (Fig. 1, B and D; Table 3). Treatment with RIF had no effect on the pharmacokinetics of WAR (Fig. 1C; Table 3).

The Metabolic Activities of Human P450 Enzymes in the Liver Microsomes. The metabolic activities of seven human P450 enzymes were determined in the liver microsomes prepared from PXB mice treated with RIF. The fold-induction of enzyme activity for each P450 isoform in the RIF-treated group is shown in Fig. 2. The metabolic activities of CYP3A4 (1′- and 4-hydroxy-TRZ), CYP2C8 (5-hydroxy- and *N*-demethyl-ROS), and CYP2C19 (4-hydroxy-MEP), whose induction was detected in the in vivo study, were significantly increased with increased doses of RIF. Although CYP2C9 induction was not detected in the in vivo study, the metabolic activity of CYP2C9 (7-hydroxy-WAR and 4′-hydroxydiclofenac) was significantly increased by RIF treatment. In addition to CYP3A4 and CYP2C enzymes, the metabolic activities of the CYP1A2, CYP2B6, and CYP2D6 enzymes were also examined. The metabolic activity of CYP2B6 (hydroxybupropion) but not CYP1A2 (acetaminophen) or CYP2D6 (dextrorphan) was increased in a dose-dependent manner by RIF.

TABLE 3

The pharmacokinetic parameters of TRZ, ROS, WAR, and MEP administered orally in cassette dosing after repeated intraperitoneal administration of RIF once daily for 4 days to the male PXB mice

Each value was determined from the data shown in Fig. 1. Data represent the mean ± S.D. of three mice.

		RIF Dose	C_{max}	$t_{1/2}$	AUC_{0-t}	AUC Decrease
		mg/kg	*ng/ml*	*h*	*ng · h/ml*	*%*
CYP3A4	TRZ	Vehicle	824 ± 92	0.733 ± 0.066	1210 ± 110	
		2	643 ± 72*	0.775 ± 0.055	650 ± 117**	46
		10	408 ± 45**	0.699 ± 0.109	561 ± 205***	54
		50	531 ± 43***	0.575 ± 0.028	346 ± 27***	71
CYP2C8	ROS	Vehicle	1970 ± 240	1.07 ± 0.13	4960 ± 770	
		2	1920 ± 210	1.10 ± 0.18	4120 ± 680	17
		10	1900 ± 350	0.911 ± 0.075	3690 ± 860	26
		50	1850 ± 330	0.772 ± 0.058	2630 ± 900*	47
CYP2C9	WAR	Vehicle	680 ± 26	ND	3830 ± 60	
		2	640 ± 161	ND	3120 ± 830	19
		10	709 ± 197	ND	3420 ± 610	11
		50	715 ± 5	ND	3160 ± 400	18
CYP2C19	MEP	Vehicle	951 ± 250	0.757 ± 0.249	1240 ± 230	
		2	955 ± 150	0.683 ± 0.144	844 ± 173	32
		10	894 ± 102	0.660 ± 0.155	876 ± 84	30
		50	730 ± 61	0.524 ± 0.120	685 ± 198*	46

ND, not determined

Statistically significant from the vehicle-treated group: * $P < 0.05$; ** $P < 0.01$; *** $P < 0.001$.

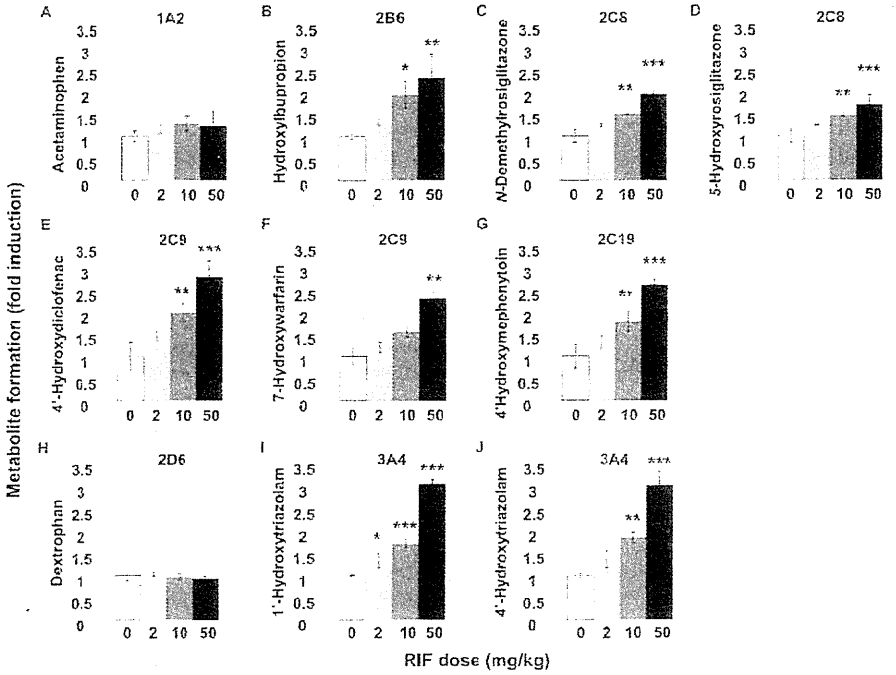

FIG. 2. The metabolic activities of P450 enzymes in the liver microsomes prepared from PXB mice. The liver microsomes were prepared from RIF- or vehicle-treated PXB mice. The activities of P450 enzymes, CYP1A2 (A), CYP2B6 (B), CYP2C8 (C and D), CYP2C9 (E and F), CYP2C19 (G), CYP2D6 (H), and CYP3A4 (I and J), were determined. The experimental conditions are summarized in Table 2. The fold induction in the RIF-treated group compared with vehicle-treated group was calculated. The metabolic activity of each of the mouse liver microsomes was determined from the means of duplicate assay. Each bar represents the mean ± S.D. of three mice. Statistically significant from the vehicle-treated group: *, $P < 0.05$, **, $P < 0.01$, and ***, $P < 0.001$.

The mRNA Expression of Human P450 Enzymes and Transporters. The mRNA expression of the seven human P450 enzymes, UGT1A1, and transporters, including MDR1 and MRP2, was evaluated in the livers of the PXB mice treated with RIF. The fold induction of mRNA expression of enzymes and transporters in the RIF-treated group is shown in Fig. 3. The magnitude of CYP3A4 induction was the largest among the P450 enzymes, followed by CYP2C8 and CYP2B6. Although the enzyme activities of CYP2C9 and CYP2C19 were increased by RIF treatment, the increase in mRNA expression was too slight to detect significant difference. No changes in the mRNA expression of CYP1A2 and CYP2D6 were observed. RIF treatment significantly increased the mRNA expression of UGT1A1, but not MDR1 and MRP2.

Discussion

In the present study, in vivo study using PXB mice, we simultaneously investigated the inductive effect of RIF on CYP3A4 and CYP2C enzymes. We demonstrated that concomitant use of RIF

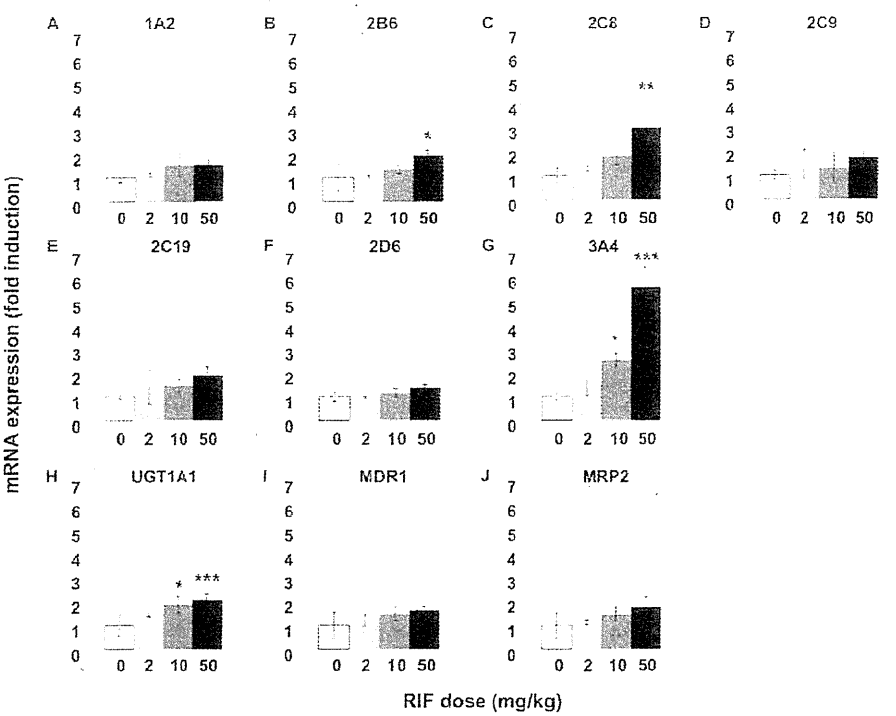

FIG. 3. The mRNA expression levels of P450 enzymes and drug transporters in the liver of PXB mice. The mRNA expression levels of CYP1A2 (A), CYP2B6 (B), CYP2C8 (C), CYP2C9 (D), CYP2C19 (E), CYP2D6 (F), CYP3A4 (G), UGT1A1 (H), MDR1 (I), and MRP2 (J) were determined by SYBR-PCR. The mRNA expression level of each gene was normalized to that of GAPDH. The fold induction in the RIF-treated group compared with vehicle-treated group was calculated. Each bar represents the mean ± S.D. of three mice. Statistically significant from the vehicle-treated group: *, $P < 0.05$, **, $P < 0.01$, and ***, $P < 0.001$.

affects the pharmacokinetics of both CYP3A4 and CYP2C substrate drugs and that the inductive effect of RIF on CYP3A4 is greater than that on CYP2C enzymes. In addition, in vitro studies using the liver samples after RIF treatment were also carried out to examine the enzyme activities of human P450s and the mRNA expression levels of human P450s, UGT, and transporters. The induction by RIF was observed in the genes whose expression levels were known to be regulated by the human PXR, but no change was observed in the genes not regulated by the PXR (CYP2D6).

To compare the pharmacokinetic data between studies conducted in humans and this study, we selected substrate drugs that have previously been reported to have DDIs with RIF in humans. In a clinical study, the AUC decreases in the P450 substrate drug with concomitant use of RIF (600 mg daily) were 46 to 78% (ROS), 57 to 85% (WAR), and 95% (TRZ) (Villikka et al., 1997; Niemi et al., 2003, 2004; Park et al., 2004). The DDI information on CYP2C19 substrate drugs is very limited, and we could only find information about the urinary excretion data for 4′-hydroxymephenytoin, the main metabolite of MEP (Zhou et al., 1990; Feng et al., 1998). The concomitant use of RIF (600 mg daily) increased the urinary excretion of 4′-hydroxymephenytoin from 1.4- to 2.8-fold (Zhou et al., 1990). Assuming that the urinary excretion amount of the metabolite reflects the metabolic clearance of MEP, the decrease in the AUC would be between 29 to 64% as a result of RIF treatment. These reported clinical data suggest that CYP3A4 is the most susceptible to induction by RIF treatment and that the magnitude of induction of CYP2C8, CYP2C9, and CYP2C19 by RIF seems to be relatively weak compared with CYP3A4. In this study using PXB mice, RIF treatment resulted in the largest AUC decrease in TRZ, followed by ROS and MEP (Fig. 1; Table 3). The response to RIF treatment observed in the PXB mice is therefore similar to that in humans.

It was unexpected that the exposure to WAR was not affected by RIF treatment, despite CYP2C9 induction in the liver microsomes (Figs. 1C and 2, E and F; Table 3). The elimination pathways of WAR other than metabolism by CYP2C9 might have made it harder to detect CYP2C9 induction in the in vivo study. In humans, WAR is mainly metabolized to the 7-hydroxyl metabolite by CYP2C9, although WAR is also metabolized to other hydroxyl metabolites by other P450 isoforms (Inoue et al., 2009). Given that the PXB mice used in the present study were derived from the hepatocytes of a single donor, the contribution of CYP2C9 to WAR metabolism in these PXB mice might not be uniformly typical of humans in general. The availability of murine P450 isoforms remaining in the liver of PXB mice could also potentially have affected the overall metabolism of WAR in the in vivo study.

We measured the metabolic activities of WAR in the liver microsomes of SCID (severe combined immunodeficiency) mice (the background strain of the PXB mice) and in pooled human liver microsomes to compare them with PXB mice (supplemental figure). The three types of hydroxyl metabolites of WAR, including 7-hydroxy-WAR, were detected in all of the microsomes. However, the 7-hydroxylation activity in the liver microsomes of PXB mice was only one fifth of that in the human liver microsomes. Therefore, the contribution of CYP2C9 to WAR metabolism in the PXB mice may have been smaller than expected. In fact, the formation of another hydroxyl WAR (M2) in the liver microsomes of SCID mice was greater than that in the human liver microsomes, although the absolute metabolic clearance was not determined (supplemental figure). The metabolic activity of murine P450s remaining in the liver could possibly make it difficult to examine CYP2C9 induction by examining the pharmacokinetics of WAR.

To investigate whether a genetic polymorphism could explain the lower CYP2C9 activity in PXB mice, the CYP2C9 genomic polymorphism was determined by Invader assay (BML, Inc., Tokyo, Tokyo) for the cryopreserved human hepatocytes (lot BD85) used in this study. Although no variant sequence was detected in the CYP2C9 gene (data not shown), real-time quantitative reverse transcription-PCR analysis revealed that the mRNA expression level of CYP2C9 in the hepatocytes was relatively low compared with that in other donor hepatocytes (data not shown). In fact, the plasma elimination of WAR in this study seems to be slower than that in the previous study using PXB mice transplanted with a different lot of human hepatocytes (Inoue et al., 2008). Therefore, the main reason for the failure to detect of CYP2C9 induction in the in vivo study was probably the low hepatic expression of CYP2C9 in the PXB mice used in this study.

In humans, a therapeutic dose of RIF (600 mg) resulted in an $AUC_{0-\infty}$ of 22,400 to 35,300 ng · h/ml (Polk et al., 2001), which was a similar range of plasma exposure as the PXB mouse receiving the 10 mg/kg RIF (M. Kakuni, unpublished data). Considering the AUC decrease of the substrate drugs in PXB mice and humans caused by RIF treatment, the inductive response in PXB mice seems to be relatively weaker than that in humans. It has been reported that CYP3A4, CYP2C8, CYP2C9, and CYP2C19 are expressed in the human intestine (Kolars et al., 1992; Läpple et al., 2003; van de Kerkhof et al., 2008). In addition, it is well known that drug metabolism by intestinal CYP3A4 affects the pharmacokinetics of orally administered drugs (Kato et al., 2003). RIF was previously reported to induce CYP3A4 not only in the liver but also in the intestine in humans (Kolars et al., 1992; van de Kerkhof et al., 2008). Therefore, the decrease in the AUC by concomitant use of RIF in the clinic is accounted for by induction of P450 enzymes both in the liver and in the intestine. In PXB mice, only the liver, but not the intestine, is humanized. Therefore, the intestinal P450 enzymes in PXB mice cannot be induced by RIF, which is a specific human PXR ligand. As a result of the lack of induction in the intestinal P450 enzymes in PXB mice, the reduction of the AUC in the PXB mice would be predicted to be smaller than that in humans. In addition, the hepatic exposure of PXB mice to RIF might be smaller than the expected level, because RIF was administered intraperitoneally, not orally, to PXB mice in this study. The relatively low exposure of the liver to RIF may have result in a weaker induction in the PXB mice.

The induction of CYP3A4 and CYP2C8, CYP2C9, and CYP2C19 by RIF in PXB mice was also demonstrated by examining the enzyme activities using typical substrates for each P450 isoform (Fig. 2). The induction of CYP2B6 in the liver microsomes was also detected (Fig. 2B). This result is consistent with the fact that the expression of CYP2B6 is regulated by the human PXR (Sinz et al., 2008). Next, we determined the mRNA expression levels of other genes, including UGT1A1, MDR1, and MRP2, whose expression levels are also under the regulation of the human PXR (Fig. 3) (Nakata et al., 2006). It was previously demonstrated that RIF led to a small increase in the mRNA expression of these genes using human hepatocytes (Nishimura et al., 2008a,b). In this study, the mRNA expression levels seemed to be slightly increased by RIF in a dose-dependent manner. Statistically significant increase was observed in the mRNA expression levels of UGT1A1 but not in those of MDR1 or MRP2 expression (Fig. 3, H–J). These results might be also attributed to the use of single donor hepatocytes as discussed above.

In the present study, we have performed a DDI study focusing on the human PXR-related induction of CYP3A4 and CYP2C enzymes simultaneously by using the cassette dosing of substrate drugs in PXB mice. We have demonstrated that the PXB mice show a similar response to humans in terms of human PXR-related P450 induction by

RIF. Because the PXB mice used in the present study were derived from the hepatocytes of a single donor, further studies are needed to generalize the present findings by performing DDI studies using PXB mice derived from the different hepatocyte donors.

Considering the magnitude of induction and its contribution to the drug metabolism in clinical situations, CYP3A4 is the most important enzyme to examine during the preclinical development of a new drug candidate. Several groups have established PXR and/or CYP3A4 humanized mice using gene knockout and transgenic techniques (Xie et al., 2000; Ma et al., 2007; Kim et al., 2008; Scheer et al., 2008; Hasegawa et al., 2011). On the other hand, the previous and present DDI studies have demonstrated that the induction of CYP2C enzymes also has a large impact on the pharmacokinetics of CYP2C substrate drugs (Niemi et al., 2003). At present, chimeric mice with a humanized liver, including the PXB mice, are only animal model available to investigate DDIs caused by the induction of CYP2C together with CYP3A4. Furthermore, several groups have reported that the drug-metabolizing profiles in PXB mice are similar to those in humans (Kamimura et al., 2010). Therefore, PXB mice seem to be a suitable animal model to examine the enzyme induction by a drug and its metabolite(s) if these are ligands for the human PXR. In conclusion, PXB mice will provide the opportunity to examine potential DDIs caused by PXR-related enzyme induction in a situation similar to that observed in humans.

Acknowledgments

We thank Tatsuya Matsumi and Dr. Saburo Sugai for supporting this research and reviewing the manuscript.

Authorship Contributions

Participated in research design: Hasegawa and Tahara.

Conducted experiments: Hasegawa, Tahara, Inoue, Kakuni, and Tateno.

Performed data analysis: Hasegawa.

Wrote or contributed to the writing of the manuscript: Hasegawa, Tahara, and Ushiki.

References

Chen Y and Goldstein JA (2009) The transcriptional regulation of the human CYP2C genes. *Curr Drug Metab* **10**:567–578.

Cui X, Thomas A, Gerlach V, White RE, Morrison RA, and Cheng KC (2008) Application and interpretation of hPXR screening data: validation of reporter signal requirements for prediction of clinically relevant CYP3A4 inducers. *Biochem. Pharmacol* **76**:680–689.

de Wildt SN, Kearns GL, Leeder JS, and van den Anker JN (1999) Cytochrome P450 3A: ontogeny and drug disposition. *Clin Pharmacokinet* **37**:485–505.

Dixit V, Hariparsad N, Li F, Desai P, Thummel KE, and Unadkat JD (2007) Cytochrome P450 enzymes and transporters induced by anti-human immunodeficiency virus protease inhibitors in human hepatocytes: implications for predicting clinical drug interactions. *Drug Metab Dispos* **35**:1853–1859.

Feng HJ, Huang SL, Wang W, and Zhou HH (1998) The induction effect of rifampicin on activity of mephenytoin 4′-hydroxylase related to M1 mutation of CYP2C19 and gene dose. *Br J Clin Pharmacol* **45**:27–29.

Hasegawa M, Kapelyukh Y, Tahara H, Seibler J, Rode A, Krueger S, Lee DN, Wolf CR, and Scheer N (2011) Quantitative prediction of human pregnane X receptor and cytochrome P450 3A4 mediated drug-drug interaction in a novel multiple humanized mouse line. *Mol Pharmacol* **80**:518–528.

Inoue T, Nitta K, Sugihara K, Horie T, Kitamura S, and Ohta S (2008) CYP2C9-catalyzed metabolism of *S*-warfarin to 7-hydroxywarfarin in vivo and in vitro in chimeric mice with humanized liver. *Drug Metab Dispos* **36**:2429–2433.

Inoue T, Sugihara K, Ohshita H, Horie T, Kitamura S, and Ohta S (2009) Prediction of human disposition toward *S-3H*-warfarin using chimeric mice with humanized liver. *Drug Metab Pharmacokinet* **24**:153–160.

Jones SA, Moore LB, Shenk JL, Wisely GB, Hamilton GA, McKee DD, Tomkinson NC, LeCluyse EL, Lambert MH, Willson TM, et al. (2000) The pregnane X receptor: a promiscuous xenobiotic receptor that has diverged during evolution. *Mol Endocrinol* **14**:27–39.

Kamiguchi N, Aoyama E, Okuda T, and Moriwaki T (2010) A 96-well plate assay for CYP4503A induction using cryopreserved human hepatocytes. *Drug Metab Dispos* **38**:1912–1916.

Kamimura H, Nakada N, Suzuki K, Mera A, Souda K, Murakami Y, Tanaka K, Iwatsubo T, Kawamura A, and Ushi T (2010) Assessment of chimeric mice with humanized liver as a tool for predicting circulating human metabolites. *Drug Metab Pharmacokinet* **25**:223–235.

Kanebratt KP and Andersson TB (2008) HepaRG cells as an in vitro model for evaluation of cytochrome P450 induction in humans. *Drug Metab Dispos* **36**:137–145.

Kato M, Chiba K, Hisaka A, Ishigami M, Kayama M, Mizuno N, Nagata Y, Takakuwa S, Tsukamoto Y, Ueda K, et al. (2003) The intestinal first-pass metabolism of substrates of CYP3A4 and P-glycoprotein-quantitative analysis based on information from the literature. *Drug Metab Pharmacokinet* **18**:365–372.

Katoh M, Matsui T, Nakajima M, Tateno C, Soeno Y, Horie T, Iwasaki K, Yoshizato K, and Yokoi T (2005a) In vivo induction of human cytochrome P450 enzymes expressed in chimeric mice with humanized liver. *Drug Metab Dispos* **33**:754–763.

Katoh M, Watanabe M, Tabata T, Sato Y, Nakajima M, Nishimura M, Naito S, Tateno C, Iwasaki K, Yoshizato K, et al. (2005b) In vivo induction of human cytochrome P450 3A4 by rifabutin in chimeric mice with humanized liver. *Xenobiotica* **35**:863–875.

Kim S, Dinchuk JE, Anthony MN, Orcutt T, Zoeckler ME, Sauer MB, Mosure KW, Vuppugalla R, Grace JE Jr, Simmermacher J, et al. (2010) Evaluation of cynomolgus monkey pregnane X receptor, primary hepatocyte, and in vivo pharmacokinetic changes in predicting human CYP3A4 induction. *Drug Metab Dispos* **38**:16–24.

Kim S, Pray D, Zheng M, Morgan DG, Pozzano JG, Zoeckler ME, Chimalakonda A, and Sinz MW (2008) Quantitative relationship between rifampicin exposure and induction of Cyp3a11 in SXR humanized mice: extrapolation to human CYP3A4 induction potential. *Drug Metab Lett* **2**:169–175.

Kolars JC, Schmiedlin-Ren P, Schuetz JD, Fang C, and Watkins PB (1992) Identification of rifampin-inducible P450IIIA4 (CYP3A4) in human small bowel enterocytes. *J Clin Invest* **90**:1871–1878.

Lapple F, von Richter O, Fromm MF, Richter T, Thon KP, Wisser H, Griese EU, Eichelbaum M, and Kivistö KT (2003) Differential expression and function of CYP2C isoforms in human intestine and liver. *Pharmacogenetics* **13**:565–575.

LeCluyse EL (2001) Pregnane X receptor: molecular basis for species differences in CYP3A induction by xenobiotics. *Chem Biol Interact* **134**:283–289.

Luo G, Guenthner T, Gan LS, and Humphreys WG (2004) CYP3A4 induction by xenobiotics: biochemistry, experimental methods and impact on drug discovery and development. *Curr Drug Metab* **5**:483–505.

Ma X, Shah Y, Cheung C, Guo GL, Feigenbaum L, Krausz KW, Idle JR, and Gonzalez FJ (2007) The PREgnane X receptor gene-humanized mouse: a model for investigating drug-drug interactions mediated by cytochromes P450 3A. *Drug Metab Dispos* **35**:194–200.

Nakata K, Tanaka Y, Nakano T, Adachi T, Tanaka H, Kaminuma T, and Ishikawa T (2006) Nuclear receptor-mediated transcriptional regulation in Phase I, II, and III xenobiotic metabolizing systems. *Drug Metab Pharmacokinet* **21**:437–457.

Niemi M, Backman JT, Fromm MF, Neuvonen PJ, and Kivistö KT (2003) Pharmacokinetic interactions with rifampicin: clinical relevance. *Clin Pharmacokinet* **42**:819–850.

Niemi M, Backman JT, and Neuvonen PJ (2004) Effects of trimethoprim and rifampin on the pharmacokinetics of the cytochrome P450 2C8 substrate rosiglitazone. *Clin Pharmacol Ther* **76**:239–249.

Nishimura M, Koeda A, Morikawa H, Satoh T, Narimatsu S, and Naito S (2008a) Comparison of inducibility of multidrug resistance (MDR)1, multidrug resistance-associated protein (MRP)1, and MRP2 mRNAs by prototypical microsomal enzyme inducers in primary cultures of human and cynomolgus monkey hepatocytes. *Biol Pharm Bull* **31**:2068–2072.

Nishimura M, Koeda A, Shimizu T, Nakayama M, Satoh T, Narimatsu S, and Naito S (2008b) Comparison of inducibility of sulfotransferase and UDP-glucuronosyltransferase mRNAs by prototypical microsomal enzyme inducers in primary cultures of human and cynomolgus monkey hepatocytes. *Drug Metab Pharmacokinet* **23**:45–53.

Park JY, Kim KA, Kang MH, Kim SL, and Shin JG (2004) Effect of rifampin on the pharmacokinetics of rosiglitazone in healthy subjects. *Clin Pharmacol Ther* **75**:157–162.

Polk RE, Brophy DF, Israel DS, Patton R, Sadler BM, Chittick GE, Symonds WT, Lou Y, Kristoff D, and Stein DS (2001) Pharmacokinetic interaction between amprenavir and rifabutin or rifampin in healthy males. *Antimicrob Agents Chemother* **45**:502–508.

Raney JL, Moeller L, Dunn K, Allen SW, Strom S, and Lasker JM (2002) Expression and induction of CYP2C P450 enzymes in primary cultures of human hepatocytes. *J Pharmacol Exp Ther* **302**:475–482.

Scheer N, Ross J, Rode A, Zevnik B, Niehaves S, Faust N, and Wolf CR (2008) A novel panel of mouse models to evaluate the role of human pregnane X receptor and constitutive androstane receptor in drug response. *J Clin Invest* **118**:3228–3239.

Shin HC, Kim HR, Cho HJ, Yi H, Cho SM, Lee DG, Abd El Aty AM, Kim JS, Sun D, and Amidon GL (2008) Comparative gene expression of intestinal metabolizing enzymes. *Biopharm Drug Dispos* **30**:411–421.

Sinz M, Wallace G, and Sahi J (2008) Current industrial practices in assessing CYP450 enzyme induction: preclinical and clinical. *AAPS J* **10**:391–400.

Strom SC, Davila J, and Grompe M (2010) Chimeric mice with humanized liver: tools for the study of drug metabolism, excretion, and toxicity. *Methods Mol Biol* **640**:491–509.

Sugihara K, Kitamura S, Yamada T, Ohta S, Yamashita K, Yasuda M, and Fujii-Kuriyama Y (2001) Aryl hydrocarbon receptor (AhR)-mediated induction of xanthine oxidase/xanthine dehydrogenase activity by 2,3,7,8-tetrachlorodibenzo p-dioxin. *Biochem. Biophys Res Commun* **281**:1093–1099.

Tateno C, Yoshizane Y, Saito N, Kataoka M, Utoh R, Yamasaki C, Tachibana A, Soeno Y, Asahina K, Hino H, et al. (2004) Near completely humanized liver in mice shows human-type metabolic responses to drugs. *Am J Pathol* **165**:901–912.

van de Kerkhof EG, de Graaf IA, Ungell AL, and Groothuis GM (2008) Induction of metabolism and transport in human intestine: validation of precision-cut slices as a tool to study induction of drug metabolism in human intestine in vitro. *Drug Metab Dispos* **36**:604–613.

Villikka K, Kivistö KT, Backman JT, Olkkola KT, and Neuvonen PJ (1997) Triazolam is ineffective in patients taking rifampin. *Clin Pharmacol Ther* **61**:8–14.

Xie W, Barwick JL, Downes M, Blumberg B, Simon CM, Nelson MC, Neuschwander-Tetri BA, Brunt EM, Guzelian PS, and Evans RM (2000) Humanized xenobiotic response in mice expressing nuclear receptor SXR. *Nature* **406**:435–439.

Zhou HH, Anthony LB, Wood AJ, and Wilkinson GR (1990) Induction of polymorphic 4′-hydroxylation of *S*-mephenytoin by rifampicin. *Br J Clin Pharmacol* **30**:471–475.

Address correspondence to: Dr. Maki Hasegawa, Kyowa Hakko Kirin Co., Ltd., 1188 Shimotogari, Nagaizumi-cho, Sunto-gun, Shizuoka, 411-8731, Japan. E-mail: maki.hasegawa@kyowa-kirin.co.jp

J Med Dent Sci 2012; 59: 43-52

Original Article

Hepatic stellate cells mediate differentiation of dendritic cells from monocytes

Rie Ozeki[1], Sei Kakinuma[2], Kinji Asahina[1),*], Keiko Shimizu-Saito[1], Shigeki Arii[2], Yujiro Tanaka[2] and Hirobumi Teraoka[1]

1) Department of Pathological Biochemistry, Medical Research Institute, Tokyo Medical and Dental University, 2-3-10 Kandasurugadai, Chiyoda-ku, Tokyo 101-0062, Japan
2) Graduate School of Medical and Dental Sciences, Tokyo Medical and Dental University, 1-5-45 Yushima, Bunkyo-ku, Tokyo 113-8519, Japan
**) Present address: Department of Pathology, Keck School of Medicine, University of Southern California, Los Angeles, USA*

Background We have previously reported that human umbilical cord blood (UCB)-nucleated cells differentiate into hepatocyte-like cells when cultured in a 5-cytokine cocktail medium. We further found that UCB cells rather differentiated into dendritic-shaped cells by coculture with a human stellate cell (HSC) line, LI90.
Methods Monocytes from UCB and adult peripheral blood were cocultured with LI90 or rat primary HSCs in a cell-culture insert. Monocytes were also cultured with LI90-conditioned medium containing secreted factors, which were analyzed by a cytokine array.
Results In the coculture with LI90, resulting dendritic-shaped cells from monocytes expressed dendritic cell (DC) markers and activated allogeneic T cells, indicating that the dendritic-shaped cells were DCs. LI90 in the cytokine cocktail medium secreted various inflammatory factors, such as granulocyte-macrophage colony-stimulating factor (GM-CSF) and interleukin-4. Fibroblast growth factor-2 in the cytokine cocktail was responsible for GM-CSF production from LI90 cells and for differentiation of monocytes into DCs in the LI90 coculture. Moreover, the coculture of monocytes with activated HSCs derived from damaged rat liver induced the differentiation of DCs, whereas quiescent HSCs derived from normal liver scarcely induced such a change.
Conclusion These results suggest that activated HSCs are involved in differentiation of monocytes into DCs in the liver.

Key words: hepatic stellate cell, dendritic cell, GM-CSF, FGF-2, the space of Disse

Introduction

In systemic immune system, dendritic cells (DCs) are the most potent antigen-presenting cells and appear to be the major cell type capable of initiating a primary T cell-dependent immune response.[1] Immature DCs are highly specialized antigen-capturing cells characterized by high expression of CD1a and mannose receptors involved in antigen uptake and phagocytosis.[2] Immature DCs reside in most tissues and are recruited to inflamed sites. After capturing and processing antigens, DCs migrate to the T-cell areas of secondary lymphoid organs and stimulate naïve T cells. In *in vitro* experiments, differentiation of DCs from monocytes is recapitulated in the presence of granulocyte-macrophage colony-stimulating factor (GM-CSF) and interleukin (IL)-4.[3,4] Tumor necrosis factor (TNF)-α and prostaglandin E_2 (PGE_2) further induce the maturation step of DCs and expression of CD80, CD83 and CD86 *in vitro*.[5,6]

The liver is continuously exposed to a wide range of antigens carried by portal blood from the intestine. In the liver, DCs reside in the sinusoids[7] and play a pivotal

Corresponding Author: Hirobumi Teraoka PhD.
Graduate School of Medical and Dental Sciences, Tokyo Medical and Dental University, Tokyo, 113-8519, Japan.
Tel: +81-3-5803-5811 Fax: +81-3-5803-0212
E-mail: hteraoka.pbc@mri.tmd.ac.jp
Received October 12 ; Accepted November 11, 2011

role not only in immune responses but also in tolerance against antigens.[8] Thus, clarifying the recruitment and function of hepatic DCs is critical to understanding the hepatic immune system. The antigen-capturing DCs in the liver are derived from the bone marrow and presumably enter the lymphatic capillaries in the portal area and translocate into the hepatic lymph nodes.[9,10] Cabillic et al.[11] reported that the hepatic environment influences monocyte differentiation into DCs. Although Kupffer cells are known to contribute to recruitment of DCs in the liver,[12] it remains elusive how differentiation, recruitment and translocation of DCs are regulated by different types of liver cells.

Hepatic stellate cells (HSCs) store vitamin A droplets in their cytoplasm and reside in the space of Disse.[13] HSCs secrete hepatocyte growth factor (HGF) and pleiotrophin and induce proliferation of hepatocytes during liver regeneration.[14] Upon liver injury, HSCs are activated and participate in the progression of liver fibrosis.[15,16] The activated HSCs lose their vitamin A storage capacity; express α-smooth muscle actin (SMA); secrete cytokines such as fibroblast growth factors (FGFs); and participate in the remodeling of extracellular matrices. HSCs regulate inflammation by secretion of chemokines, including monocyte chemotactic protein (MCP)-1 and macrophage inflammatory protein 2.[17] In addition, HSCs serve as liver-resident antigen-presenting cells.[18] However, it is not known whether HSCs influence immune responses via DCs during liver injury.

We have previously reported that human umbilical cord blood (UCB)-nucleated cells differentiate into hepatocyte-like cells when cultured in a cytokine cocktail medium containing FGF-1, FGF-2, leukemia inhibitory factor (LIF), stem cell factor (SCF) and HGF.[19] During the course of the study, we found that UCB cells rather differentiated into DC-like cells by coculture with a human HSC line, LI90. To test whether HSCs regulate differentiation of DCs in the liver, we further clarified mechanism of HSC-dependent differentiation of DCs from monocytes. In the present study, we found that HSC-induced DC-like cells are functional and that the cultured LI90 cells and activated primary HSCs secrete several cytokines and induce differentiation of DCs from monocytes. These results suggest that HSCs participate in immune responses via induction of DCs during the liver injury.

Materials and Methods

Coculture of UCB or peripheral blood cells with LI90

UCB samples from full-term deliveries were collected after informed consent in writing. The study protocol was approved by the ethical committees of Medical Research Institute, Tokyo Medical and Dental University and Kanto Medical Center NTT East Corporation. Adult peripheral blood was obtained from healthy volunteers after informed consent in writing. Nucleated cells in the UCB samples were obtained using 6% hydroxyethyl starch (Nipro Co., Osaka, Japan) as previously described.[19] To obtain mononuclear cells from UCB or peripheral blood, blood samples were diluted with phosphate buffered saline (PBS) containing 2% bovine serum albumin and 0.6% citrate and layered on top of a Lymphoprep™ (Nycomed, Oslo, Norway). Mononuclear cells were isolated by density centrifugation, and monocytes were obtained by adhesion selection.[20] Human UCB cells were also purchased from RIKEN Bioresource Center (Tsukuba, Japan). UCB cells (2×10^7 cells/well) or monocytes (5×10^5 cells/well) were cultured in a 6-well plate (Becton Dickinson, Franklin Lakes, NJ, USA) coated with 0.1% gelatin in Dulbecco's modified Eagle's medium (Sigma, St. Louis, MO, USA) supplemented with 15% fetal bovine serum (JRH Biosciences, Lenexa, KS, USA), 2 mM L-glutamine, 25 mM HEPES, 100 U/ml penicillin, 100 μg/ml streptomycin, 0.25 mg/ml amphotericin B, and 300 μM monothioglycerol (DMEM/FBS medium) at 37°C in a 5% CO_2 atmosphere. The culture medium was supplemented with human recombinant cytokines including 20 ng/ml FGF-1 (Invitrogen, Grand Island, NY, USA), 10 ng/ml FGF-2 (Invitrogen), 10 ng/ml LIF (Chemicon, Temecula, CA, USA), 10 ng/ml SCF (R&D Systems, Minneapolis, MN, USA) and 10 ng/ml HGF (a kind gift from Mitsubishi Chemical Co., Tokyo, Japan). An LI90 cell line was kindly provided by Dr. T. Matsuura (The Jikei University School of Medicine, Tokyo, Japan).[21] LI90 was seeded on the membrane of cell culture insert (Becton Dickinson) that is composed of transparent polyethylene terephthalate membrane (0.45 μm). The LI90 in the insert was cocultured with UCB or peripheral blood cells on the 6-well plates up to day 21. For maturation of DCs, the culture continued in the medium supplemented with 1 ng/ml PGE_2 (Sigma) and 25 ng/ml TNF-α (Invitrogen) for additional 2 days. The conditioned medium was collected 7, 14 and 21 days after culture of LI90 with the 5-cytokine cocktail upon